IMAGE QUALITY ENHANCEMENT

ROBERT W. BRAINARD
GEORGE N. ORNSTEIN, PhD

FOREWORD

This study was initiated by the Behavioral Sciences Laboratory of the Aerospace Medical Research Laboratories, Aerospace Medical Division, Wright-Patterson Air Force Base, Ohio. The research was conducted by the Columbus Division of North American Aviation Incorporated, Columbus, Ohio under Contract No. AF33(616)-7996. Dr. George N. Ornstein, Engineering Chief, Advanced Systems Research, directed the research for North American Aviation, and Mr. Robert W. Brainard served as Project Leader for North American Aviation. Dr. Aaron Hyman of the Presentation of Information Branch, Human Engineering Division, was the contract monitor for the Aerospace Medical Research Laboratories. The work was performed in support of Project No. 7183, "Psychological Research on Human Performance," and Task No. 718302, "Fundamental Parameters in Perception." The research sponsored by this contract was initiated in December 1962 and completed in February 1964.

This technical report has been reviewed and is approved.

WALTER F. GRETHER
Technical Director
Behavioral Sciences Laboratory

ii

ABSTRACT

A technique for enhancing the quality of imagery was investigated. The technique consists of obtaining a video signal from a transparency and adding to this signal its first and/or second derivative(s). The efficacy of the technique was evaluated by comparing imagery produced by the video signal and its derivative(s) with imagery produced by the video signal alone. The imagery investigated consisted of standard test patterns and aerial photographs. The processed test patterns were quantitatively analyzed to determine the resolution, contrast and acutance of the imagery. The results indicate: (1) differentiation enhances image quality, as indicated by the resolution, contrast and acutance metrics, (2) greatest enhancement is produced by operations which include second-order differentiation, and (3) the least enhancement is produced by first-order differentiation. The aerial photographic imagery shows the same enhancing effects as those obtained with the test patterns.

TABLE OF CONTENTS

LIST OF ILLUSTRATIONS

LIST OF TABLES

INTRODUCTION

The successful performance of many weapon systems depends upon the availability of information regarding the location and identity of enemy targets. Such information is often obtained from a display on which is presented an image of the area of interest. The task of the human in this situation is to visually search the display in order to locate and identify significant cultural and terrain features.

A prime problem frequently encountered by the human in this situation is the lack of satisfactory image quality. The image, in the course of its acquisition and display, is subject to myriad degrading factors, including: the undulatory nature of radiation, atmospheric turbulence, contrast attenuation, sensor resolution, dynamic range and system noise. The effect of these factors is uniformly in the direction of increasing the homogeneity of the spatial-luminance distribution, which is the image. Instead of being sharply separated, adjacent luminance areas will be connected by diffuse spatial-luminance transitions. Thus, contrast will be reduced and image elements, which would otherwise be resolvable, will become indistinguishable.

The sheer numerosity and diversity of the debilitating factors just enumerated indicates that some degree of image degradation is unavoidable in an operational environment. The need for reducing the extent of image quality degradation in this situation leads directly to the investigation of image enhancement techniques. The remainder of this report presents the progress made to date in the investigation of one such technique. Specifically, this presents (a) the background rationale for the enhancement technique, (b) a description of the experimental apparatus, and (c) the results from a preliminary investigation of the technique.

BACKGROUND

Factors in Image Quality

Historically, "resolution" has been regarded as the index of image quality. However, since resolution merely designates the minimum size detail which can be separated, it provides no information as to the clarity and sharpness with which larger details are reproduced. "From a study of resolution and detail contrast characteristics of photographic and television images it has long been apparent that the sharpness of an image has no fixed relation to the limit of resolution of the system . . ." (See ref 26, p 231). It has been found that image sharpness is, instead, a function of the shape and steepness of the edge-gradients of the image (ref 22). In attempting to develop a quantitative index of sharpness, Higgins and Jones (ref 12) investigated edge-gradients such as those shown in figure 1. One index investigated was the

1

maximum gradient, which occurs near the center of the curve. As a measure of sharpness this index failed to distinguish an edge-gradient having a sweeping toe and shoulder from one with an abrupt toe and shoulder; the latter produces a higher degree of perceived sharpness. An index based on the
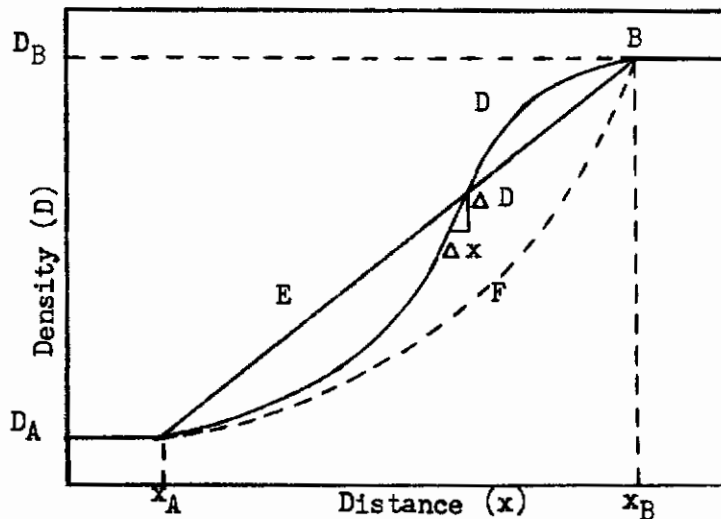

Figure 1

Distribution of Density in
Image of Knife-edge

average gradient between two points (eg points A and B in figure 1) was also unsatisfactory in that it failed to distinguish between gradients like E (or F) and D which have the same average gradients. The final index selected correlated very highly (r = 0.994) with observer judgments of sharpness. This index, termed "acutance," was defined as the mean-square gradient divided by the density difference, or,

$$G_x^{-2} = \frac{\sum (\Delta D_i / \Delta x_i)^2}{n} \Big/ DS,$$ (1)

where n is the number of $\Delta D_i / \Delta x_i$ measurements and DS is the density difference between points A and B.

2

Subsequent research has shown that for a more satisfactory index of image "definition"*, it is necessary to combine resolution with acutance. (See ref 13.) An empirical expression derived from a particular experiment suggested the formula,

$$\text{Definition} = \text{Acutance} \cdot 1 - e^{-kR^2} \,, \tag{2}$$

where k is a constant peculiar to the particular experiment, and R is resolution. The precise relationship between acutance and resolution in their joint influence on definition remains to be worked out. In addition to these factors, image graininess has also been found to influence sharpness (ref 27). At present, image definition is believed to be influenced principally by four factors -- sharpness, resolution, graininess and tonal reproduction. However, of these four factors, sharpness (measured in terms of the edge-gradient) is believed to be most significant in determining image definition. (See ref 22.)

Importance of Edge-Gradient in Visual Performance

Considerable empirical evidence is available which shows directly the significant role of image edge-gradients in human visual perception and performance. If, for example, the edge-gradient is made sufficiently shallow, the difference between adjacent luminance areas in an image will not be detectable, even though the brightness differential (contrast) between the two areas is well above threshold. (See ref 21.) Moreover, by properly shaping the edge-gradient, the apparent contrast may be made to oppose that of the actual spatial-luminance distribution of the image, and in some cases to produce apparent contrast where none actually exists. It has been concluded from findings of this nature that perceived contrast is ". . . formed over the boundary of an object . . ." (ref 21, p 115), ie, over the spatial-luminance transition connecting adjacent areas.

The basic role of edge-gradients in perception is further illustrated by the results from retinal image stabilization investigations. When the small involuntary eye movements, which occur under normal viewing conditions, are prevented from producing motion of the retinal image, the whole field appears uniform in spite of actual luminance variations across the field. (See refs 4, 25.) It has been stated that the disappearance of perceived differences ". . . could be described as the progressive washing out of the contours of the image . . ." (See ref 16, p 741). Riggs concludes that ". . . continuous involuntary motion of the eyes has one clearly demonstrated function, that of preventing the . . . disappearance . . . of contours . . ." (See ref 24, p 16). The effect of image stabilization can, however, be offset by introducing a nonstabilized edge into a stabilized field. When this is done perception of luminance differences across the entire field occur even though all areas of the image other than the edge are stabilized. (See ref 3.)

---

*Defined as the clarity with which details are reproduced.

3

The importance of the edge-gradient for human performance is well illustrated by results from a series of studies investigating photointerpretation. (See refs 6, 7, 10.) For example, the efficiency with which a display is searched is significantly impaired when the edge-gradient is reduced by blurring the image or by introducing differently shaped apertures. Specifically, the duration of the visual fixations increases and the distance between fixations decreases, as the edge-gradients are diffused. The net result of these two effects is that a smaller proportion of the total display is examined per unit time. The magnitude of these effects is indicated in figure 2, in which the relative amount of display area searched per unit time is plotted as a function of the angular width of the blur distribution around the edge-gradient.
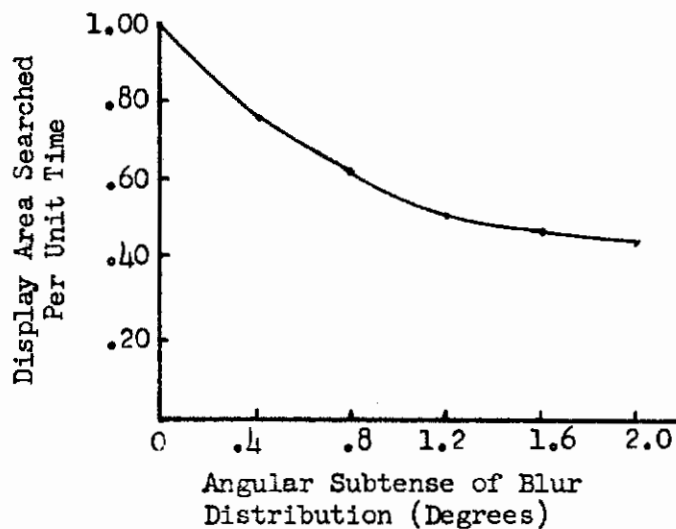

Figure 2

Influence of Edge-Gradient Diffusion
on Search Efficiency

Other aspects of human performance are detrimentally affected by edge-gradient diffusion. Typically, the identifiability of objects will be significantly reduced; target detection will also be effected, but to a lesser degree. (See ref 8.) Of particular importance is the usual finding from such studies that both speed and accuracy of performance is impaired and that the two performance measures are highly correlated (eg, ref 14).

4

The evidence reviewed above establishes the basic role of edge-gradients in both image quality and visual performance. The ability to extract information from an image ". . . depends in large measure on the ability to perceive borders . . ." (ref 21, p 112), and the perception of borders depends significantly on the nature of the edge-gradient defining the border. Since a reduction in the slope of image edge-gradients is unavoidable in any operational environment and, as a result of such image degradation, human performance is consistently impaired, an approach to image quality enhancement which is based upon the steepening of edge-gradients is suggested. The rationale for a particular technique by which edge-gradients may be steepened is presented in the following section.

RATIONALE FOR ENHANCEMENT TECHNIQUE

The optical properties of the human eye are such that the image on the retina is degraded relative to the image entering the eye. No matter how sharp the edge-gradient between adjacent luminance areas may be, the distribution of illuminance on the retina will be spread or diffused. The spread introduced by the eye derives from (1) diffraction of light by the pupillary aperture, (2) spherical and chromatic aberrations of the optical system, and (3) scattering of the image light b the dioptric media. The resulting diffusion of the image has been referred to, historically, as the "blur circle" and more recently as the "spread function" of the visual system. (Measurements and estimations of the magnitude of the diffusion, or spread of a point or line image vary from about 3 to 16μ.) (See refs 28, 29.)

In spite of the diffusing effects of the eye, the retinal image will under many conditions be perceived as being sharp and distinct. For example, if an observer views a sharp-edged, bipartite field (see figure 3a) the retinal image will have both a reduced slope and a more gradual asymptote. However, the perception of the field is quite different; the edge-gradient is perceived as steeper than the retinal image would indicate, and as having a peak and depression at the top and bottom, respectively, of the spatial-luminance plot. These relations are shown in figure 3b.
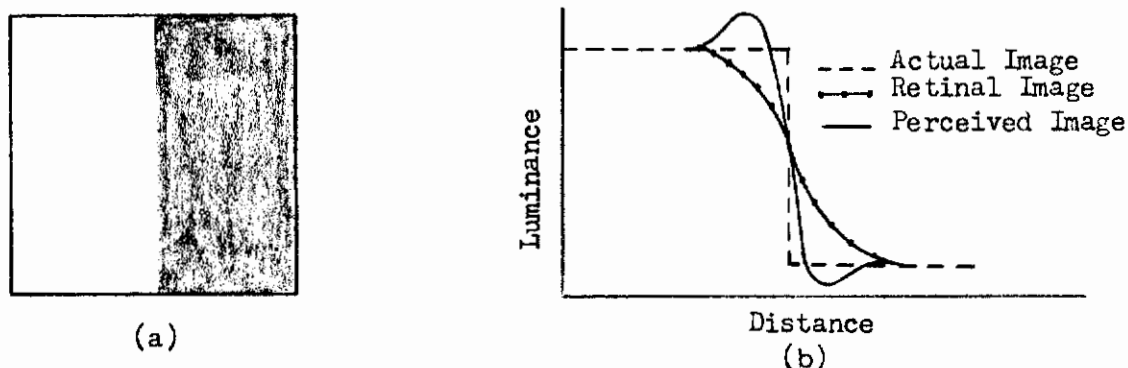

(a)

(b)

- - - Actual Image
·—·—· Retinal Image
——— Perceived Image

Luminance

Distance

Figure 3

Perception of a Bipartite Field

5

This phenomenon was apparently first noticed by Mach (ref 19) in 1865. He suggested then that its effect was describable as a second derivative correction applied to the retinal image. The equation proposed was,

$$r(x) = \alpha \log \frac{e(x)}{\beta} \pm \frac{\gamma}{e(x)} \frac{d^2 e(x)}{dx^2} \qquad (3)$$

where x is the axis along the surface of the retina, r is the perceived (or apparent) brightness, e is the retinal illuminance, and α, β and γ are constants.* (Mach noted, too, that the first derivative of the spatial-luminance distribution has little or no effect on perception, a finding which has been confirmed by Ludvigh.) (See ref 18.)

Mach's hypothesis was recently investigated by O'Brien (using a difference equation approach in view of the finite spacing of the retinal mosaic.) He concludes from empirical studies that an ". . . analysis of the qualitative features of contours observed in relation to external changes in intensity points to a process of contour enhancement by a second-difference correction . . . Regions of high positive (second difference) correction corresponded to regions of positive enhancement in the subjective perception and negative corrections to negative enhancement." (See ref 21, p 119)**

The similarity of the effects between the degrading processes influencing a displayed image and those occurring within the eye, suggests the use of an enhancement technique for the inanimate sensing system similar to that employed by the human to compensate for the diffusion introduced by his optical system. Specifically, if the derivative of the image is obtained and then subtracted from the image, the operation should act to reduce the spread of the edge-gradients, ie, to sharpen them. In consequence, this operation will result in an improvement of the effective resolution of the system over that which would be obtained without the operation. Furthermore, the effective contrast (formed over the edge-gradient) of the image will be improved. Thus, the differentiation "correction" operation offers a technique by which image quality can seemingly be enhanced through an improvement in the important quality parameters of acutance, resolution and contrast. The possibility of performing the required differentiation operations and the expected enhancement effects were first enumerated in the excellent paper by Kovasznay and Joseph. (See ref 15.)

---

*An analogous phenomenon has been observed in the eye of the Limulus (horseshoe crab) which has been interpreted as a mechanism for enhancing the detection of contours. (See ref 28.) Recently, v. Bekesy has proposed a "neural unit" which consists of an area of sensation surrounded by a refractory area of inhibition to explain a similar phenomenon which occurs in the skin and the organ of Corti (ref 21). A recent paper has shown the underlying relationships among the various models proposed for this phenomenon. (See ref 2.)

**For a discussion of possible mechanisms underlying this phenomenon, see references 5, 9 and 11.

The remainder of this report summarizes the progress made to date in the investigation of the derivative enhancement technique. Briefly, the necessary experimental apparatus (described in the following section) was constructed and evaluated, and various imagery subjected to the differation operation. The results of densitometry analyses of these materials, together with the imagery, are included in the final section of this report.

APPARATUS

The Electro-Optical Signal Processing System (ESPS) used in this research program was originally designed as a general purpose research device; specific modifications and extensions of the general apparatus were required to permit the execution of the research reported herein. The following description of the device represents the system configuration employed in the present program. A brief functional description of the system will be followed by a more detailed description of key system operations and components.

Functional Description of the ESPS

A block diagram of the ESPS is presented in figure 4. The drive for the flying spot scanner and the synchronized television monitor is supplied from the two sine-wave oscillators. The signal generated by one oscillator drives the vertical yokes of both the flying-spot scanner and the monitor, while the horizontal yokes are driven by the other oscillator. The forcing function supplied by the two oscillators drives the flying-spot (focused by an intervening lens) so as to scan a photographic transparency. The light intensity of the flying-spot, after passing through the transparency, is proportional to the transmissivity of the particular point of the transparency through which it passed. The transmitted light is then focused by the condensing lens onto the sensing element of the photo-multiplier. Here, the light is converted to an electrical signal, the voltage of which is linearly related to the intensity of the light transmitted by the photographic transparency.

Once in an electrical form, the following operations of specific interest may be performed on the signal:

1. First order differentiation
2. Second order differentiation
3. Signal transmission without differentiation
4. Amplification of any of the signals resulting from the above operations.
5. All possible combinations of the above operations.

Thus, the output signal, ψ, may be specified as consisting of a weighted composite of three operations

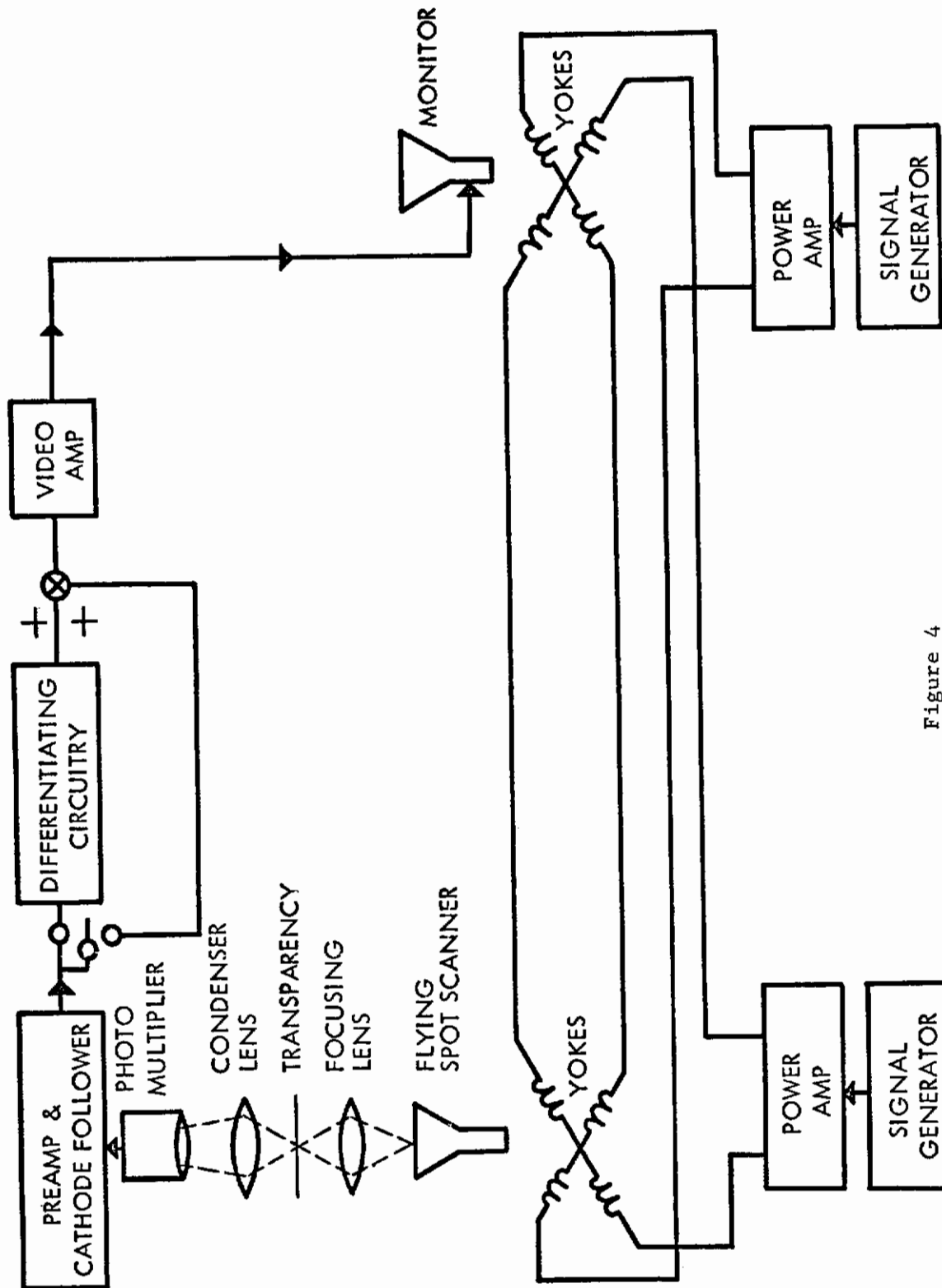$$\psi = K_o \theta + K_1 \frac{d\theta}{dt} + K_2 \frac{d^2\theta}{dt^2} \qquad (4)$$

7

Figure 4

Schematic of the Electro-Optical
Signal Processing System

8

where the K's represent amplification factors (weights), θ represents the undifferentiated signal, and $\frac{d}{dt}$ represents the time derivative.

From the differentiating, amplifying and summing circuitry, the signal, ψ, passes to the monitor grid where it modulates the intensity of the scanning beam so as to produce a tonal image on the face of the TV monitor.

Detailed Description of ESPS

In this section, the detailed characteristics of the principal components and operations of the ESPS will be described and discussed under the headings of Scanning Mode, Optical Sub-system and Differentiation Network.

Scanning Mode

The manner in which an image is scanned has considerable influence upon the quality and appearance of the final picture obtained on the TV monitor. This is especially true if such operations as differentiation of the image are to be performed. In conventional TV, scanning is horizontal from left to right (and top to bottom) across the face of the tube. With such a scanning mode, the edge of an object, say at right angles to the direction of scan, will be affected quite differently by differentiation than if the same edge were placed parallel to the direction of scan. To minimize this and other effects of a unidirectional scan, a multidirectional scanning pattern was employed, the principal characteristics of which will now be described.

Scan Pattern. The scan patterns of both the flying-spot scanner and the monitor were produced by the superposition of two independent forcing signals supplied by two audio oscillators. A sinusoidal signal (voltage) from one of the oscillators was applied to the horizontal deflection yokes. The second oscillator provided another sinusoidal signal of the same amplitude as the first, but having a slightly different frequency, which was simultaneously applied to the vertical deflection yokes. The pattern of scan produced by the combination of such signals is called a "Lissajous" figure.*

The path taken by the flying spot in drawing the Lissajous scan is given by

$$x = A \sin \omega t, \text{ and} \tag{5}$$

$$y = A \sin (\omega + \alpha) t \tag{6}$$

---

*Named for the 19th century French physicist who investigated these figures through the use of a pair of tuning forks.

where A is the amplitude of the signal, ω is the angular frequency (in radians per sec), and $\propto$ is the difference between the two angular frequencies (in radians per sec). The resulting pattern will be enscribed within a square with sides of length 2A. An illustration of a Lissajous figure is given in figure 5; this figure was generated by a "vertical" sinusoidal signal of 10 cps in combination with a "horizontal" signal of 9 cps.* In constructing figure 5, the (x,y) position of the flying-spot was computed at the end of each .001 second interval. Thus, the variation in the distance separating successive points in the figure represents the relative differences in spot velocity which occur in the process of generating the figure.

Frame Rate. If an integral number of horizontal cycles of the forcing signal occurs in exactly the same time as an integral number of vertical cycles, the flying spot will describe the same closed pattern repeatedly, ie, the pattern will be strictly periodic, provided the ratio of the signal frequencies is a rational number. Accordingly, the time, T, required to draw a single, complete Lissajous pattern (ie, the frame time) is,

$$T = \frac{2\pi n}{\omega} = \frac{2\pi(n+k)}{(\omega + \propto)} = \frac{2\pi(n+k)-2\pi n}{(\omega + \propto)-\omega} = \frac{2\pi k}{\propto} \tag{7}$$

where n is the number of full cycles made by the lower frequency sine wave in drawing a complete Lissajous, and k, an integer, is the number of cycles by which the two frequencies differ, and $\propto$ is the frequency difference. Note that changing $\propto$ produces proportional changes in T. For example, if the frequency difference $\propto$ is increased by a factor of 2, T is decreased by a factor of 2. Such a change in $\propto$ would produce a wider separation between successive scan lines and thus a shorter frame time.

Small amounts of (inherent) drift in the oscillators supplying the forcing signals will vary the frame rate slightly since $\propto$, the frequency difference, is the key factor in determing T. Providing such drift is small, no loss in image quality is incurred nor are the filtering operations appreciably affected. In fact, the contrary effects will be produced; "gaps" between scan lines will be filled and points in the image will be scanned from a multitude of slightly different directions. Each of these effects, within limits, will act to improve the apparent and actual quality of the final TV picture. In the present study a small order of drift, averaging approximately 0.2 cycles per frame, was recorded. The recorded frequency drifts were random in direction and were not cumulative.

---

*The actual frequencies used in the present study were 1025 (cps) and 1023 (cps). Figure 5 is based upon frequencies of 9 and 10 cps in order to reduce the number of intersecting lines and thereby increase the clarity of the illustration.
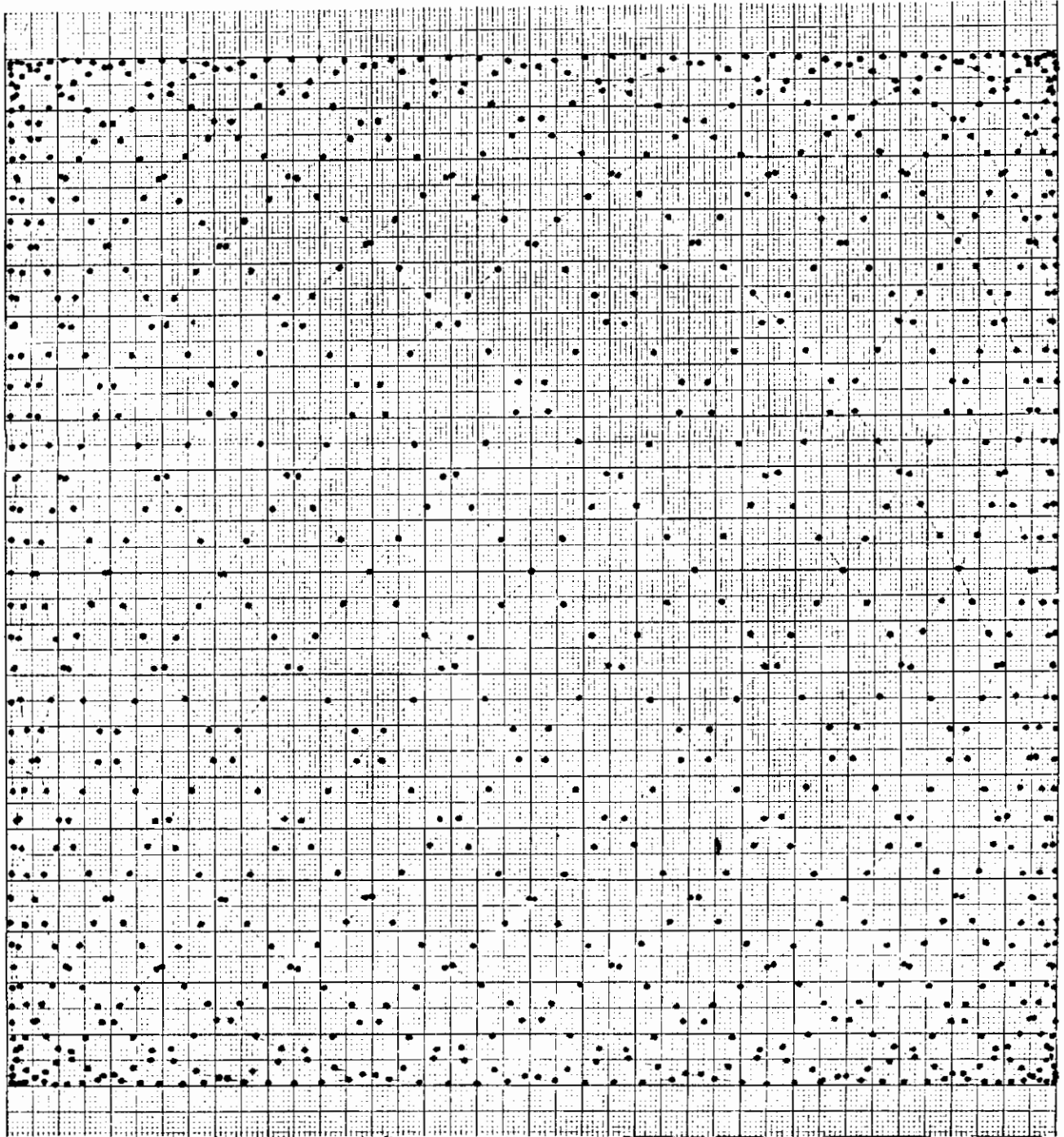
10

Figure 5

Illustration of Lissajous Scan Mode

11

It was found empirically that with the sine wave frequencies selected for study (ie, approximately 1024 cps), a camera exposure of 10 to 15 sec would yield an image (transparency) of the picture on the TV monitor which was generally free of scan lines. Transparencies free of scan lines were desired for densitometry purposes, in that the presence of scan lines would have interfered with the assessment of the effects of the differentiation operations.

Scanning Velocity and Orthogonality

Operationally, two important properties of a scan system are the velocity of the scan and the directions of scan through any point in the raster. To accomplish an undistorted* mapping from the spatial-luminance domain to the frequency-amplitude domain, the velocity of scan should be constant during the entire scanning operation. Further, to permit the determination of the spatial derivative, successive passings through any given point should be such that the directions of scan are at right angles. This orthogonality should be maintained over the entire area being scanned.

Neither of the above properties is fully realized by a Lissajous mode of scan. However, as will be shown below, the two properties are approximately realized over a sizeable portion of raster area.

The velocity of the flying-spot at any point in the scan domain may be obtained by differentiating equations (5) and (6) respectively, yielding

$$\dot{x} = \omega A \cos \omega t$$

$$\dot{y} = (\omega + \alpha) A \cos (\omega + \alpha) t$$

The velocity of the spot is therefore given by

$$V = (\dot{x}^2 + \dot{y}^2)^{1/2} = A \{ \omega^2 (1 - \sin^2 \omega t) + (\omega + \alpha)^2 [1 - \sin^2(\omega + \alpha) t] \}^{1/2}$$

$$V = [\omega^2 (A^2 - x^2) + (\omega + \alpha)^2 (A^2 - y^2)]^{1/2} \tag{8}$$

For a given ω and α, the velocity of the scanning spot varies with its momentary position in drawing the Lissajous figure. It can be seen that the maximum velocity, V_{max}, occurs at the precise center of the Lissajous figure where x=y=0 and $V_{max} = [\omega^2 A^2 + (\omega + \alpha)^2 A^2]$. The minimum velocity (ie, zero) occurs at the extreme corners of the pattern, where $x^2 = y^2 = A^2$. On the perimeter of the scan pattern, midway between any two adjacent corners, the spot velocity drops to approximately 70% of V_{max}. These relationships are

---

*Due to scanning operations.

shown in figure 6. The solid line in this figure represents the relative velocity from the center of the scan pattern (x = y = 0) to the midpoint of a side of the pattern; the total distance involved is A which has been set at 1 for these calculations. The broken line represents the relative velocity from the center along the diagonal to a corner; the total distance involved here is $\sqrt{2A}$.
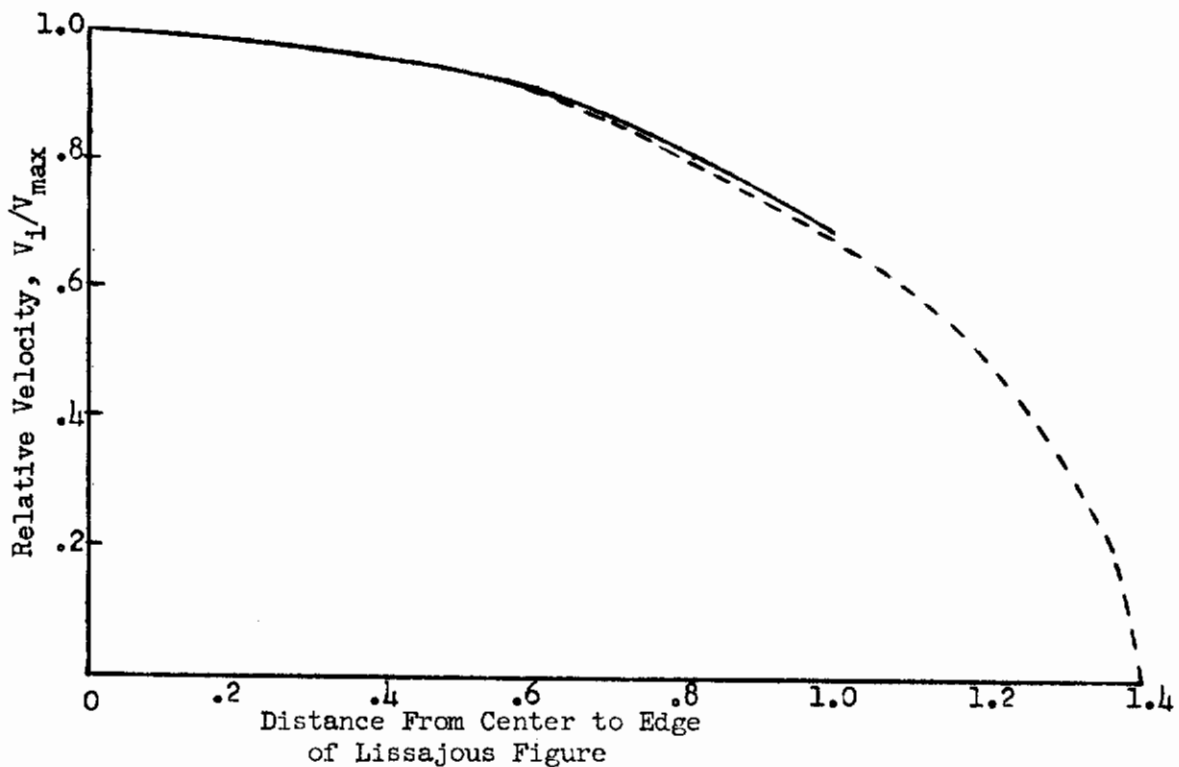

Figure 6

Relative Velocity of Flying-Spot in Generating the Lissajous Figure

As noted above, the scan system should provide scanning directions which are orthogonal to each other. However, as illustrated in the Lissajous figure (figure 5), orthogonal scanning directions are not maintained across the entire figure. The extent to which the two scan paths, through a given point, fail to exhibit this property can be directly calculated. Consider, first, the angle between the two scan paths as the midpoint of a horizontal side of the Lissajous figure is approached from the center. The slope, m_1, of one of the scan paths with respect to the horizontal is given by

13

$$m_1 = \frac{dy}{dx} = \frac{(\omega + \alpha) \cos (\omega + \alpha)t}{\omega \cos \omega t}$$

Setting $\sin \omega t = x = 0$,

$$m_1 = \pm \frac{(\omega + \alpha)}{\omega} \cos (\omega + \alpha)t$$

$$= \pm \frac{(\omega + \alpha)}{\omega} \sqrt{1 - \sin^2 (\omega + \alpha)t},$$

and $m_1 (0, y)$
$$= \pm \frac{(\omega + \alpha)}{\omega} \sqrt{1 - y^2}$$

The slope, m_2, of the second scan path with respect to the horizontal is found to be identical to slope m_1. The angle, θ, included between the two straight lines of slopes, m_1 and m_2 is the angular separation between the two scan directions. Figure 7 presents θ as a function of the distance from the center of the Lissajous figure to its side.

The angular separation of the scan directions along a diagonal may be computed in a similar manner. Setting $y = x$ (ie, dropping A, $\sin \omega t = \sin(\omega + \alpha)t$),

$$m(x,y) = \pm \frac{(\omega + \alpha)}{\omega}$$

That is, along a diagonal the two scan paths maintain the same angular separation 90°, and where ω and $(\omega + \alpha)$ are large or α is small, relative to ω, the scan directions approach orthogonality. This relation is shown in figure 7.

Optical Sub-System

The CRT used as the flying-spot scanner in the present system has a P16 phosphor type. The spectral emission of the P16 phosphor is concentrated in the UV and near UV, with peak emission occurring at approximately 3,700 Angstroms. Due to these emission characteristics, a UV-transmitting quartz lens system is used to focus the flying-spot onto the transparency. The lens system consists of a combination of two inch diameter quartz lens elements which together form a 5 feet f/14 system.

Completing the optical system is a pair of UV-transmitting Fresnel condensing lens mounted "back-to-back." The function of this unit is to collect the light transmitted by the transparency and bring it to a focus on the photo-sensing element of the photo-multiplier. Each of the two lens is 10 inches in diameter the lens pair has a focal length of 6 feet and an f of 0.5.
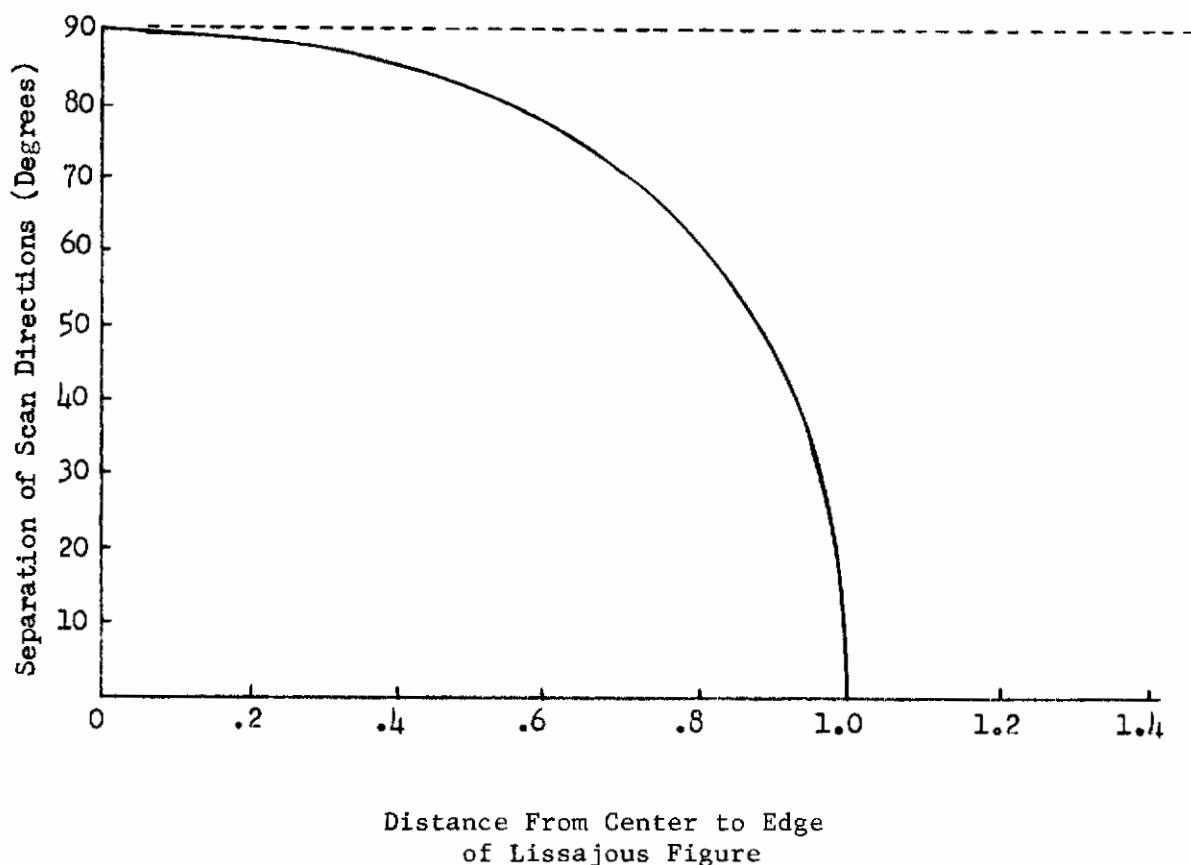
14

Figure 7

Angular Separation Between Scan Directions

The entire optical system is enclosed in an optical barrel. A small slit in this barrel permits the insertion of the transparency holder. Each element of the system can be moved along and perpendicular to the optical axis of the system; this provides for a variety of possible image scales from the same transparency, and for the scanning of selected portions of the transparency.

Differentiation Network

When the light from a scanned transparency is converted by the photo-multiplier to an electrical signal, the spatial-density distribution of the transparency is transformed to the frequency-amplitude domain. The time-varying-voltage-signal actually obtained may be viewed as comprised of a series of suitably weighted sine and cosine components. The frequencies of these components, and their coefficients, will be determined largely by the spatial-density distribution of the transparency. An analyses of the frequency

15

spectrum obtained from a transparency would reveal that high frequency components were contributed by areas of the transparency in which the spatial-density variations were rapid, namely, from edge-gradients and small objects. Conversely, low frequencies would be found to arise from areas in which the spatial-density variation is slow.

Through filtering techniques, the electrical signal obtained from scanning a transparency may be so modified that the resulting signal is approximately the same as that which would have been obtained had the signal been differentiated, in the mathematical sense.*

Various techniques are available for performing approximate differentiation operations. In this investigation, RC networks were used. A schematic of the differentiating circuitry is shown in figure 8. The output of the first RC network, e_1, which is an approximation to the first derivative, is defined as,

$$e_1(s) = \frac{\tau_1 s}{1 + \tau_1 s} \ e_i(s) \tag{9}$$

where $R_1 C_1 = \tau_1$ and s is the Laplacian operator. In the cascaded network, e_1, is the input for the second RC network, the output of which is,

$$e_2(s) = \frac{\tau_2 s}{1 + \tau_2 s} \ e_1(s), \tag{10}$$

where $\tau_2 = R_2 C_2$. The product of these two outputs constitutes the second derivative,

$$e_2(s) = \frac{\tau_1 \tau_2 s^2}{(1 + \tau_1 s)(1 + \tau_2 s)} \ e_i(s)$$
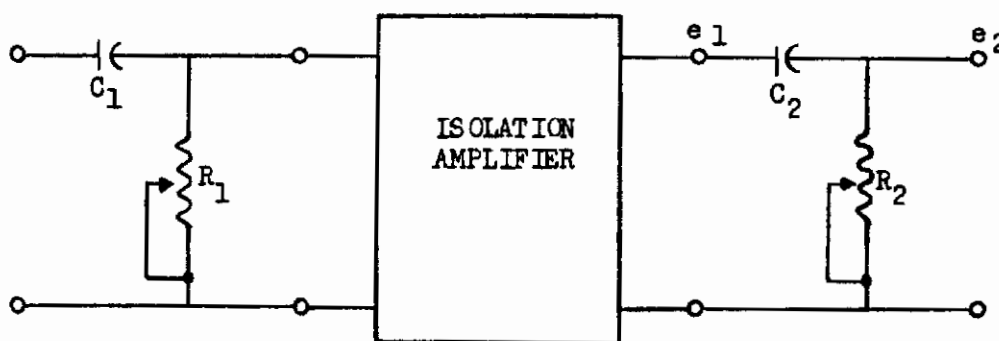
Figure 8

Differentiating Network

---

*Mathematical differentiation is a physically unrealizable operation because of the infinitesimal ($\Delta \rightarrow 0$) involved.

After differentiation, the signals (first and second derivatives) are full-wave rectified and made negative. The resulting negative derivatives may then be amplified, independently, and combined with the undifferentiated signal, which too has an independent gain control. Thus, "weighted" combinations of the three signal classes can be formed. The final image, ψ, on the TV monitor may be represented as being formed from the signal

$$\psi = K_0 \, e_i(s) + K_1 \, \frac{\tau_1 s}{1 + \tau_1 s} \, e_i(s) + K_2 \, \frac{\tau_1 \tau_2 s^2}{(1 + \tau_1 s)(1 + \tau_2 s)} \, e_i(s),$$

where the K_i represent weighting factors (amplifications) and the other terms are as defined above.

The ideal frequency-amplitude response (to a sinusoidal input) of such a circuit as that described above is shown in figure 9, together with the actual response of the circuit used in this study. The ideal and actual phase-amplitude response of the circuit is presented in figure 10. The close similarity of the two sets of curves indicates the differentiating circuitry of the ESPS approaches the ideal performance characteristics.

As shown in figure 8, the resistors in the differentiating circuit are variable. Therefore, the time constant, τ, can be varied. The effect of varying the time constant acts to shift the response of the network along the frequency scale; with a small (short) τ only higher frequencies are passed, while enlarging τ acts to expand the band of passed frequencies. The need for a selective time constant arises from the diversity of imagery to be investigated. The imagery will include various target-terrain features and will differ in regard to scale, contrast and resolution. The frequency spectrum obtained from scanning the imagery will, accordingly, differ considerably and will therefore require that different frequency-bands be passed for optimum filtering of each image.

RESULTS

The effects of differentiation operations on image quality were investigated through the use of both test patterns and aerial photographs. The materials were processed through the ESPS apparatus and photographs were taken of the resultant images. A 4 x 5 Speed Graphic Camera with a Kodak Ektar f:4.7, 127mm lens, and Super XX film was used in all the photography. This film was selected for its broad spectral response (in consonance with the broad spectral emission of the P-4 phosphor of the TV monitor) and the relatively extensive range over which its H and D curve is linear. Transmittance recordings from transparencies of the test patterns were obtained and were quantitatively analyzed to determine the acutance, contrast and resolution characteristics of the processed imagery. (The circular scanning aperture used in these operations had a diameter of 0.001 inch.) The aerial photographic materials illustrate the effects of differentiation on complex, real imagery.
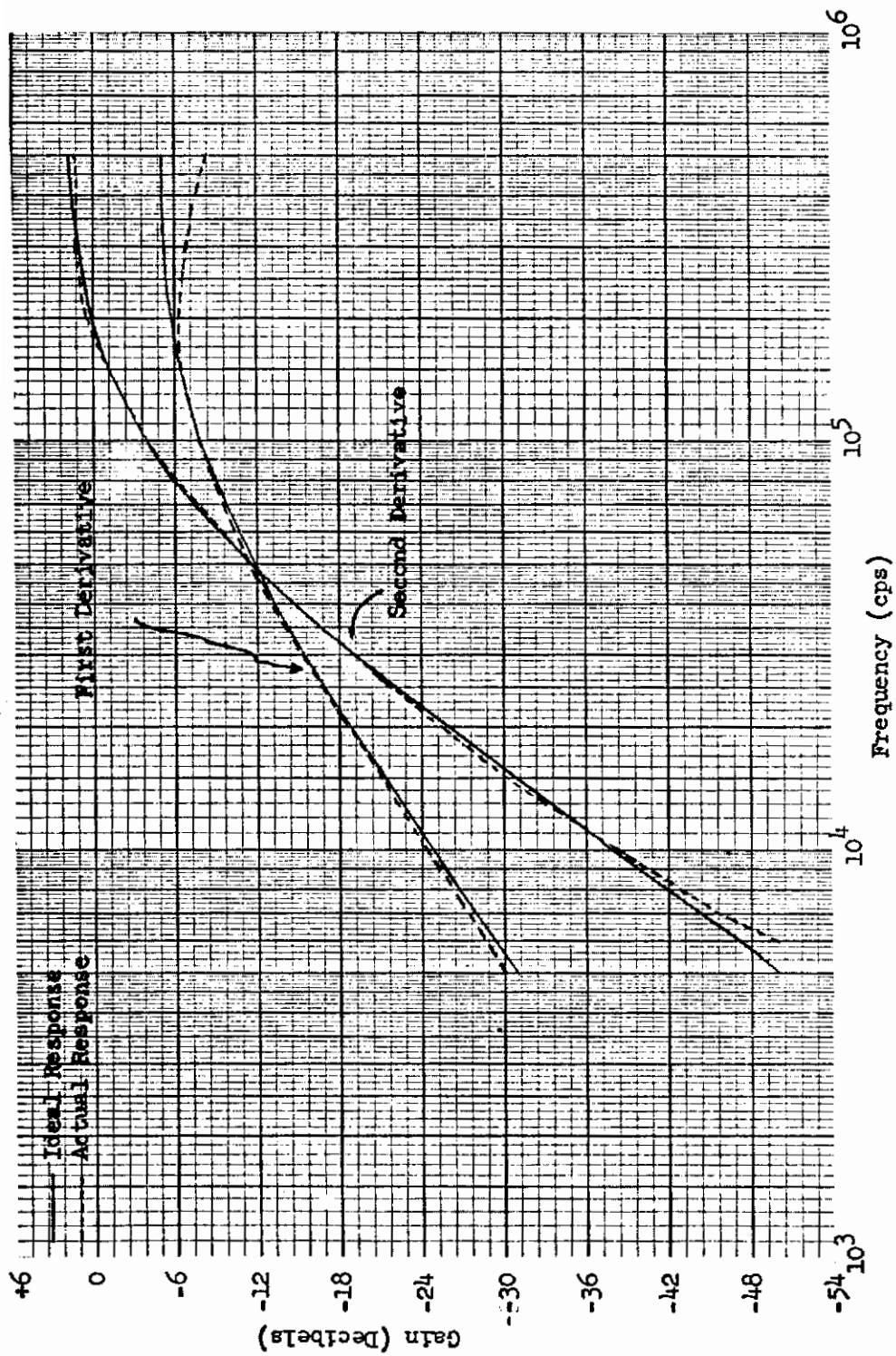
17

Figure 9

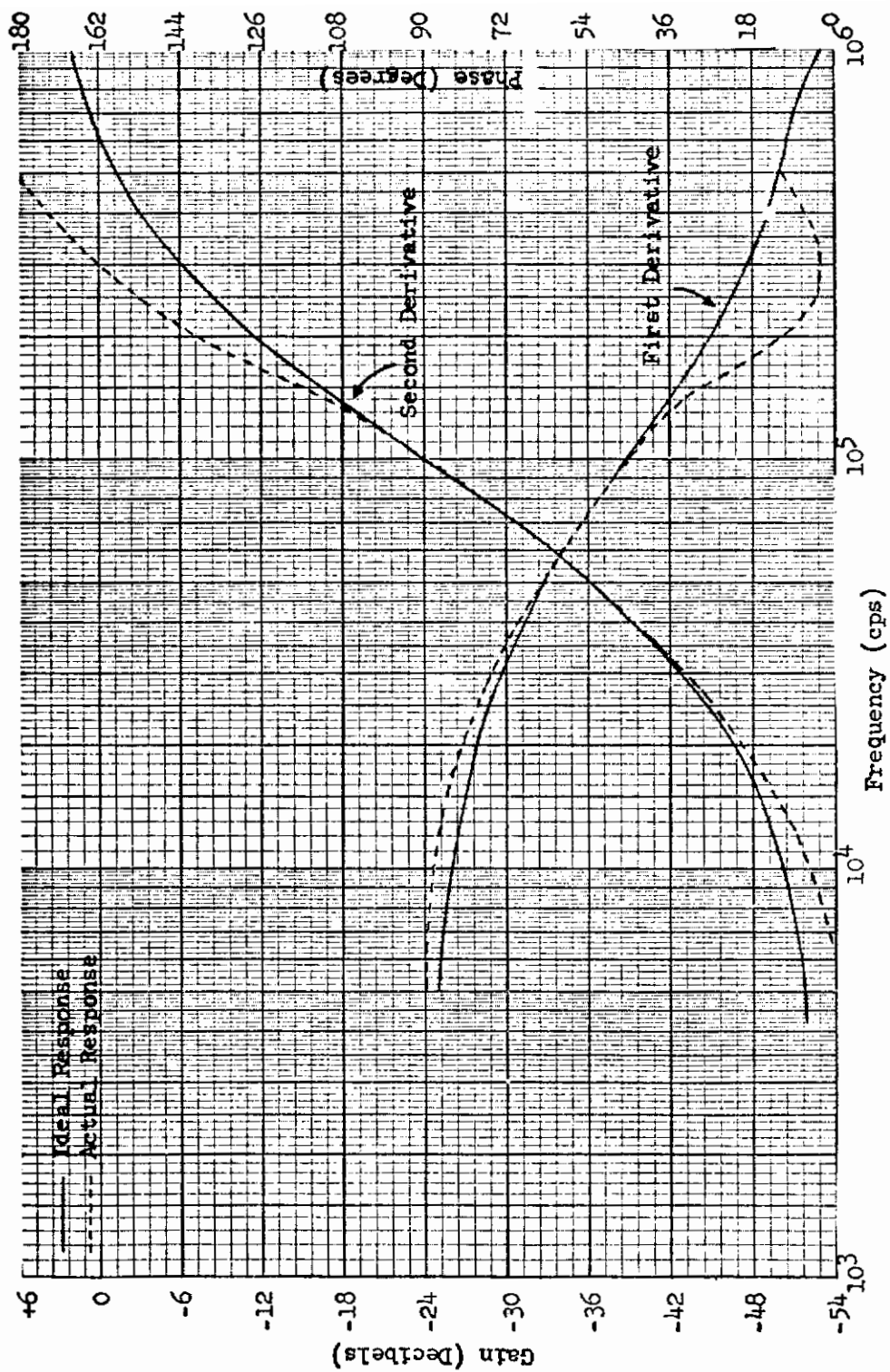Frequency-Amplitude Response of Differentiating Circuit

18

Figure 10

Phase-Amplitude Response of Differentiating Circuit

19

Test Patterns

Two test patterns were investigated: the NBS Resolution Test Chart (1952) and a sine-wave pattern marketed by Kodak Research Laboratories. The transmittance (and density) distribution of the lines comprising the NBS chart is rectangular in form, while the transmittance varies sinusoidally in the sine-wave pattern. The use of these two patterns provides fundamentally different input signals for evaluating the effects of the differentiation operations.

NBS Resolution Test Chart

Photographs* of the processed NBS pattern, as presented on the TV monitor, are shown in figure 11. Below each photograph is indicated the processing conditions involved in generating the image; θ designates the image produced by the undifferentiated video signal, while $\dot{\theta}$ and $\ddot{\theta}$ designate the negatives of the first and second derivatives, respectively, of the video signal. The relative amplification, or gain factor, in the series of photographs was varied only in the case of the second derivative, $\ddot{\theta}$, the two levels illustrated are designated by the subscripts, "H" and "L" signifying high and low gains, respectively. (The high amplification level is approximately 1.6 times that of the lower level of amplification.)

A transmittance recording through the center of the vertical set of lines was obtained for each of the photographs presented. These recordings are presented in the Appendix. From these records, acutance, contrast and resolution were calculated. The acutance was computed in accordance with equation (1); the value averaged over the first and last edge-gradients of each of the four largest line sets was calculated, and these four values were then averaged. (The Δ x unit used in the acutance calculations was 0.05 mm, but after calculation the acutance values were modified to correspond to a micron base.) The resulting acutance values are presented in table 1.

Contrast was calculated by the expression,

$$C = \frac{T_{max} - T_{min}}{T_{min}}$$

where T_{max} is the average transmittance level of the three "peaks" of the line set and T_{min} is the average transmittance of the two "valleys" separating the three lines. Resolution is defined as that number of lines/inch at which 2% contrast is obtained. Contrast as a function of the numbers of lines/inch is
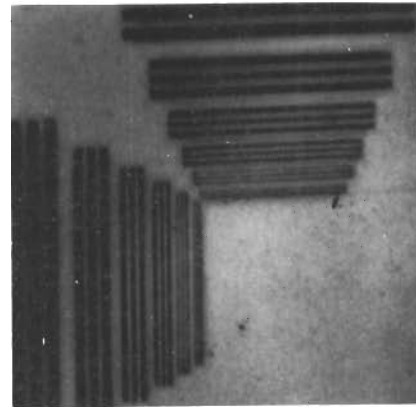
---

*Because of the previously noted nonhomogenous properties of the Lissajous scan mode, only the central 50 percent of the area of the image is included in photographs presented herein. Within this area the reduction in scanning orthogonality does not exceed 20 percent (see figure 7).
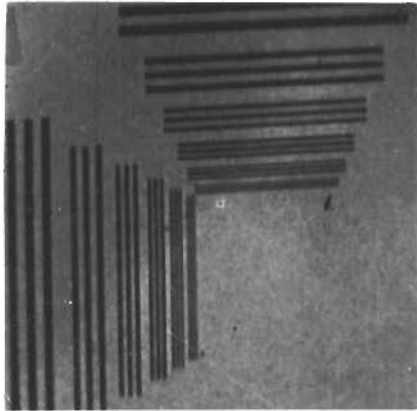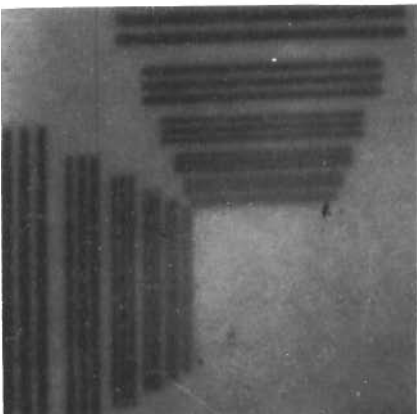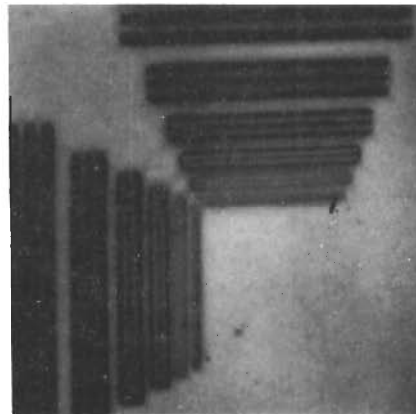
NBS No. 3 $\phi + \ddot{\theta}_H$
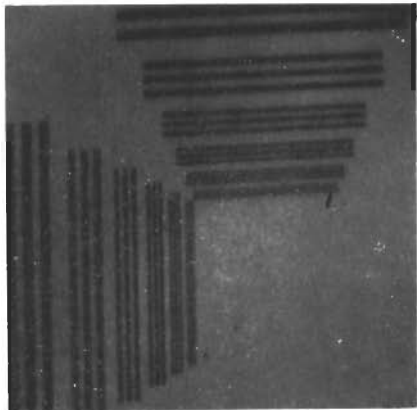
NBS No. 2 $\phi + \ddot{\theta}_L$

NBS No. 5 $\phi + \dot{\theta} + \ddot{\theta}_H$

NBS No. 1 ϕ

NBS No. 4 $\phi + \dot{\theta}$

Figure 11

NBS Photographs

21

plotted in figure 12 for each of the five processing conditions. The data do not permit the exact determination of the point of 2% contrast for any of the five processing conditions. An estimate of the 2% contrast point was obtained from an extrapolation of each plot, as shown by the broken lines in figure 12. (In some instances, the intersection point could be bracketed between the last set of resolved lines and the immediately following set of unresolved lines; this factor, as well as the curve form established by the available data points, was considered in the extrapolation.) The resulting estimates of the resolution for the various processing conditions are presented in table 1.

TABLE 1

ACUTANCE AND RESOLUTION OF THE
NBS TEST PATTERNS

Processing Condition	Mean Acutance	Resolution
θ	1.369	28.5
$\theta + \ddot{\theta}_L$	2.176	51.5
$\theta + \ddot{\theta}_H$	4.790	63.0
$\theta + \dot{\theta}$	1.780	41.0
$\theta + \dot{\theta} + \ddot{\theta}_H$	2.538	43.0

The data from the NBS chart indicate that: (1) The acutance value of the image processed under the most effective condition (high gain second derivative condition) is approximately 3.50 times greater than that obtained from the undifferentiated image, θ. The next most effective conditions were the combined first and second derivatives ($\theta + \dot{\theta} + \ddot{\theta}_H$) and the low gain second derivative condition ($\theta + \ddot{\theta}_L$), which had acutance values that were, respectively, 1.85 and 1.59 greater than the value obtained from the undifferentiated image. The least improvement (a factor of 1.30) was recorded with the first derivative operation; (2) Contrast levels were enhanced most by the second derivative high gain condition. The combined first and second derivative condition was second in effectiveness, being somewhat more effective (because of the high gain of the second derivative involved) than the low gain second derivative operation. The first order derivative condition produced an improvement in contrast for the small detail, but was increasingly ineffective for the larger detail; (3) Resolution, like acutance, was increased by all of the differentiation operations, with the greatest degree of enhancement being produced by the second derivative operations. The least amount of enhancement was, as expected, produced by first derivative operations, while an intermediate level of enhancement was produced by the combined first-and-second derivative condition.
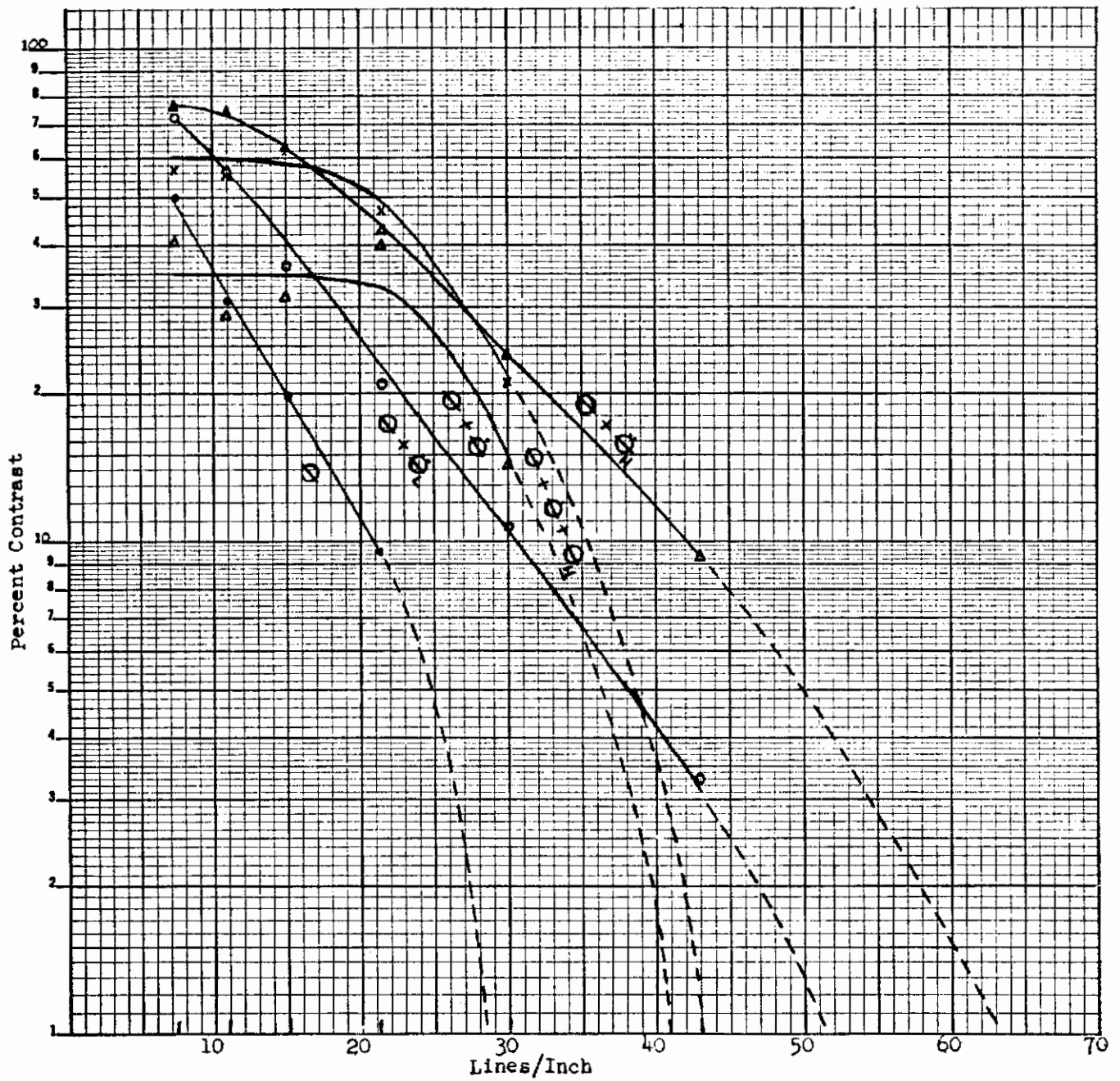
22

Figure 12

Contrast/Line Spacing Plots for NBS Patterns
Under Various Differentiation Conditions

23

Sine-Wave Test Pattern

The sine test patterns were processed under the same five conditions as the NBS charts. Photographs of the processed patterns are shown in figure 13, while the transmittance recordings obtained from each of the five transparencies are presented in the Appendix. In recording the transmittance, a sample of either three or four full cycles was recorded from each of five frequency sets in each of the photographs shown in figure 13. The first four sets recorded are indicated by the white marks to the left of the middle column; the fifth, and lowest frequency set recorded is immediately above the fourth set, ie, at the top of the middle column.

From the transmittance recordings, contrast was calculated and utilized in determining resolution as discussed above. These results are shown in figure 14. The resolution (in cycles/inch) obtained under the five different processing conditions was estimated by extrapolation, in the same manner as used in esti-mating the resolution of the NBS chart. These data are presented in table 2.*

TABLE 2

RESOLUTION OF THE SINE PATTERN

Processing Condition	Resolution
θ	32.0
$\theta + \ddot{\theta}_L$	68.5
$\theta + \ddot{\theta}_H$	74.0
$\theta + \dot{\theta}$	48.0
$\theta + \dot{\theta} + \ddot{\theta}_H$	68.0

These results are in substantial agreement with those obtained from the NBS pattern. Resolution is enhanced by all differentiation operations; the second derivative, with and without the first derivative, produces maximum enhancement, while the first derivative correction produces the least

---

*The different frequencies represented in the sine pattern obviously produce different "edge-gradients"; therefore, the acutance metric was not calculated.
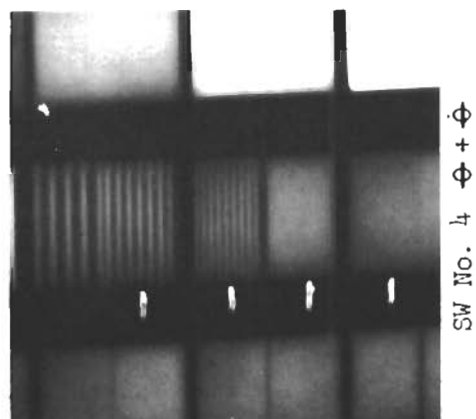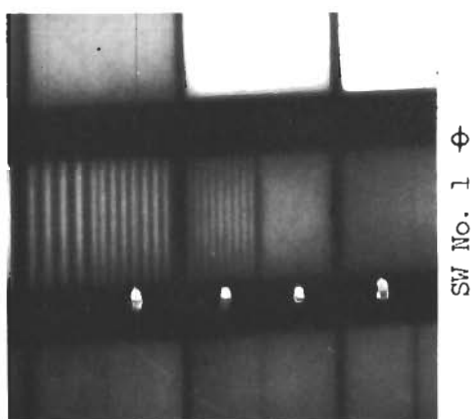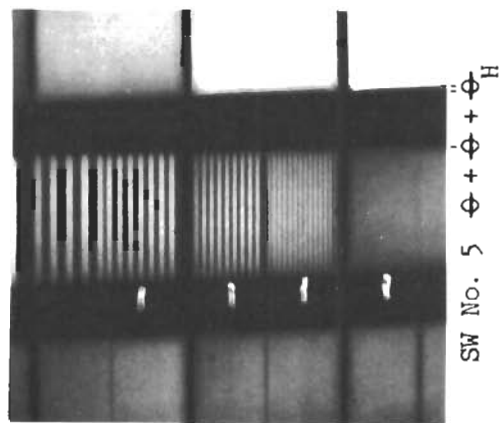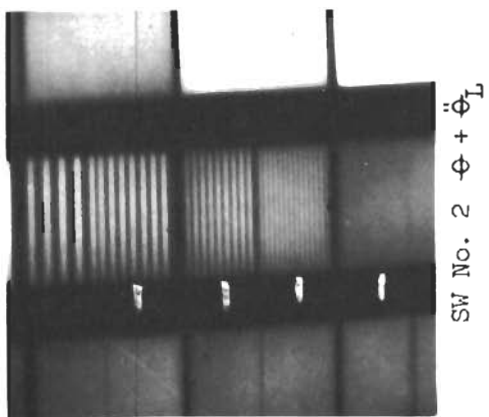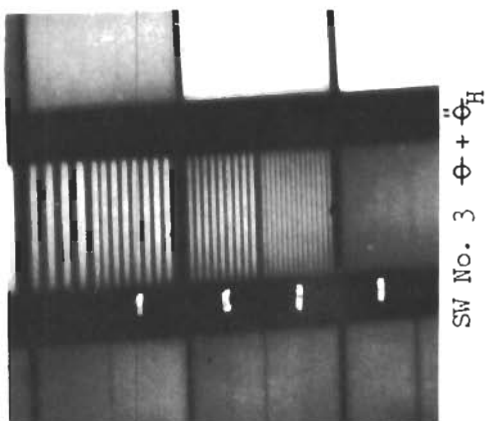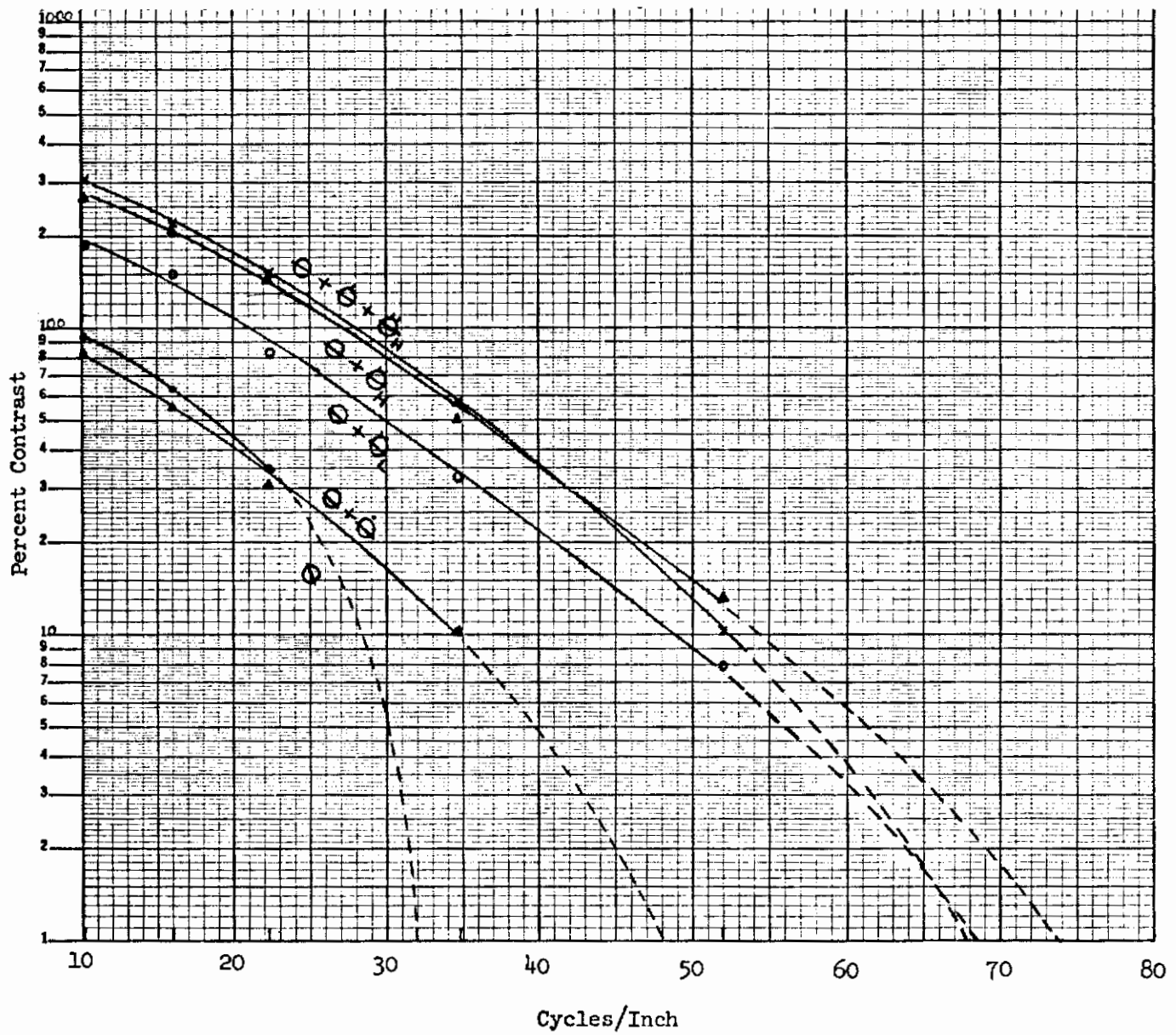
Figure 13

Sine-Wave Pattern Photographs

25

Figure 14

Contrast/Cycle Spacing Plots for Sine Patterns
Under Various Differentiation Conditions

26

effect. The combination of first and second derivative correction falls be-
tween the high and low gain second derivative conditions. The effects of
differentiation on contrast follow a similar pattern, although the first and
second differentiation combination produces a relatively greater enhancement
effect in the sine patterns than was found in the NBS materials.

Aerial Photographs

Various aerial photographs were investigated in order to assess the effects
of the differentiation operations on complex real imagery. Four aerial photo-
graphs investigated are treated in this report.

Figure 15 presents a series of photographs illustrating the effects of various
differentiation operations upon detail in real imagery (eg, aircraft engines,
wing structure, etc). The first derivative fails to enhance details; in fact,
an apparent loss of detail and form distortion are produced by the operation.
On the other hand, the second derivative appears to produce substantial enhance-
ment of detail.

Figure 16 treats an armored tank in a bushy terrain. The first three photo-
graphs illustrate the effects of the differentiation operations. With the deriva-
tive correction the turret and gun barrel of the tank appear more distinct, and
the edge-gradient connecting the tank and the background is sharpened. Similarily,
the clarity of the tank tracks and surrounding vegatation is enhanced. The last
two photographs are included to demonstrate the effects of changing the differ-
entiating time constant, τ. These photographs (5 and 6) were obtained with a
longer time constant than that used in generating photographs 2 and 3. The lower
frequencies passed by the longer time constant result in a brightness enhancement
greater than that obtained with the shorter time constant; however, the longer
time constant results in distortions of the image (see photograph No. 6).

Figure 17 treats a small nonmilitary airfield. The first photograph in
this figure was taken under a low-gain undifferentiated condition. The second
photograph was taken under a high-gain undifferentiated condition. Attention is
directed to the improved contrast and resolution resulting from only the gain
change. The third photograph was taken under a condition of low-gain with
second derivative added. This photograph may be compared with the second
photograph to obtain an appreciation of the relative effectiveness of and the
different phenomena intrinsic in the differentiation and amplification operations.
Although gain amplification above increases contrast, resolution is left rela-
tively unchanged; the addition of this second derivative, however, increases
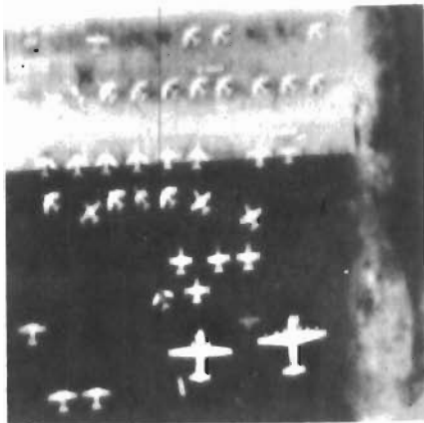both contrast and resolution.

Figure 18 parallels figure 17 in showing the relative effects of gain
versus differentiation enhancement. The "target" of interest in this figure
is a group of eight oil storage tanks located in the upper lefthand quadrant of
each photograph. The first photograph was taken under a low-gain undifferentiated
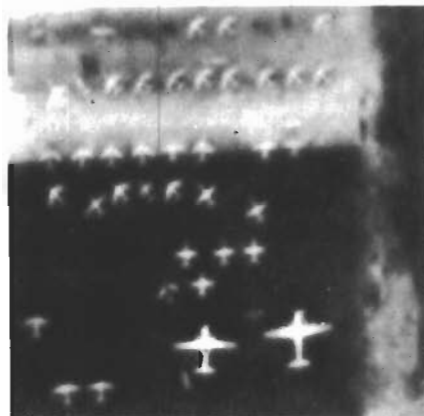
27

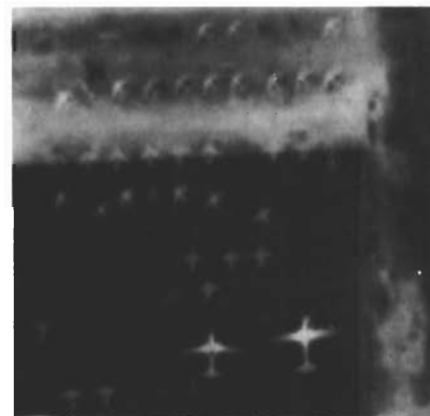No. 3 $\phi + \ddot{\phi}_H$

No. 2 $\phi + \ddot{\phi}_L$

No. 1 ϕ
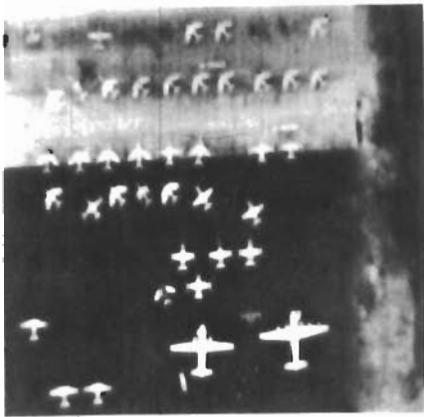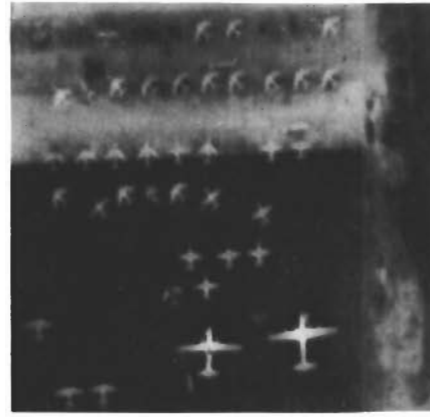
No. 6 $\phi + \dot{\phi} + \ddot{\phi}_H$
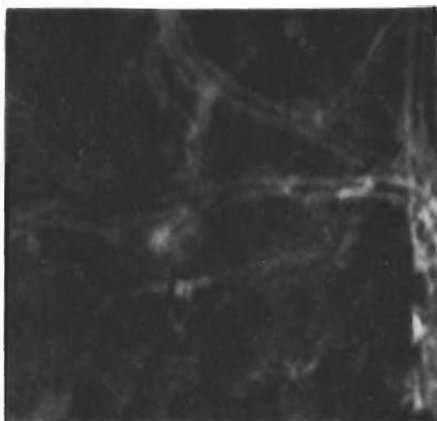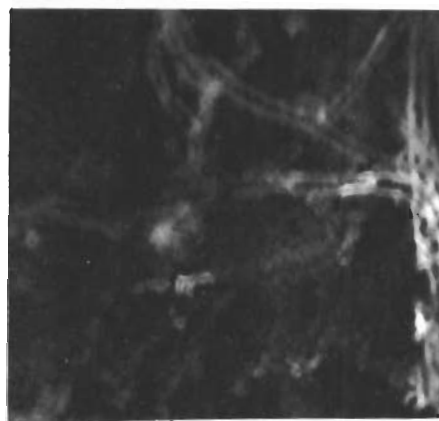
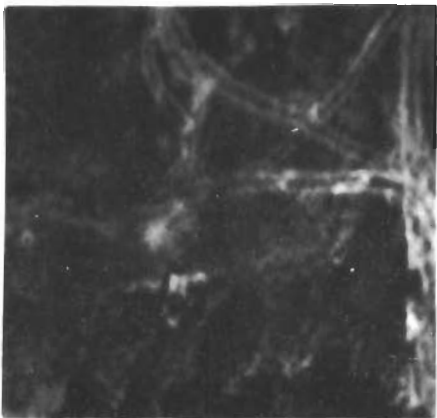No. 5 $\phi + \dot{\phi} + \ddot{\phi}_L$

No. 4 $\phi + \dot{\phi}$

Figure 15

Parked Aircraft

28
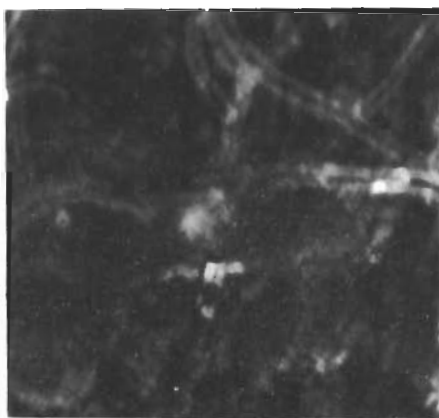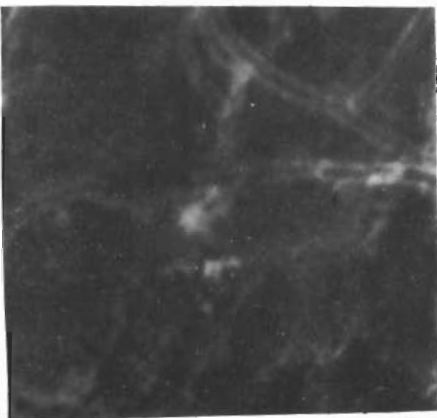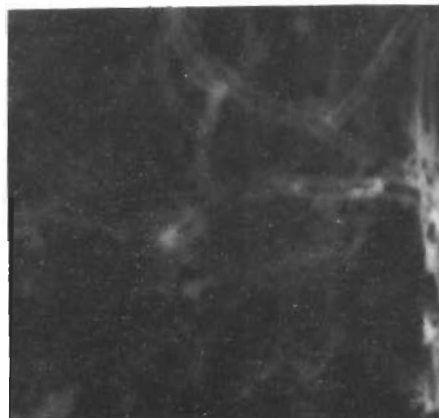
No. 3 $\phi + \dot\phi + \ddot\phi_H$

No. 6 $\phi + \dot\phi + \ddot\phi_H$

No. 2 $\phi + \ddot\phi_H$

No. 5 $\phi + \ddot\phi_H$

No. 1 ϕ

No. 4 $\phi + \phi$

Figure 16
Armored Tank

29

No. 1 ϕ_L

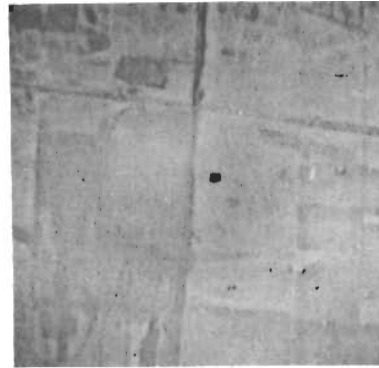No. 2 ϕ_H
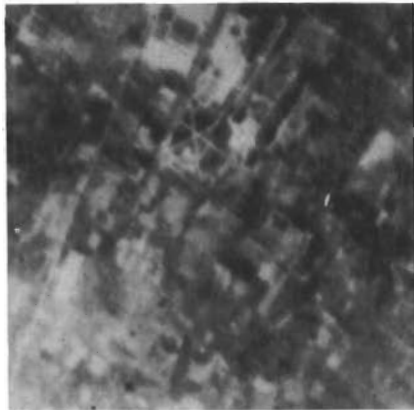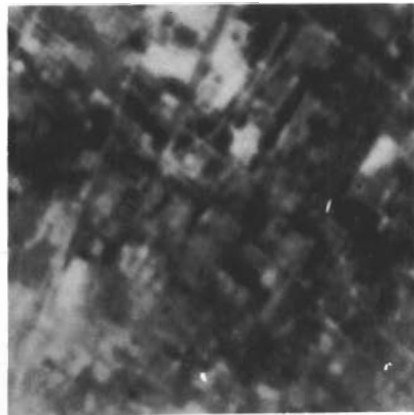
No. 3 $\phi_L + \phi_H$

Figure 17
Airfield

30

No. 2 $\dot{\Theta}_H$

No. 1 Θ_L
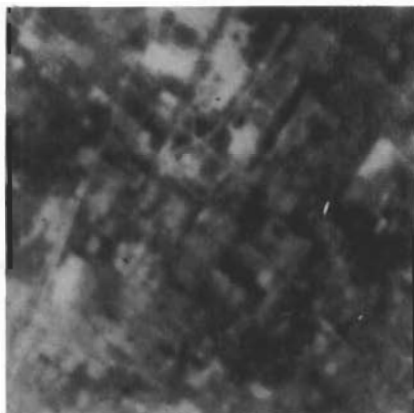
No. 4 $\ddot{\Theta}_H$

No. 3 $\Theta_L + \ddot{\Theta}_H$

Figure 18

Oil Storage Tanks

31

condition. The second photograph was taken under a high-gain undifferentiated condition. As above, attention is directed to the improved contrast and resolution resulting from only the gain change. The third photograph, taken under a condition of low gain with second derivative added, may be compared with the second photograph as was done in figure 17. The fourth photograph included in figure 18 is that of the pure second derivative signal which was added to photograph 1 to produce photograph 3.

DISCUSSION AND CONCLUSIONS

The enhancement techniques investigated in this study act to increase, or sharpen, the spatial-density gradients of the image. Basically, all the techniques investigated involve: (1) sensing the spatial-density gradients, (2) generating a signal which is, in some sense, proportional to the gradient, and (3) subtracting the latter from the original image gradients. The techniques investigated herein differ only in respect to the form of the signal which is generated, and subtracted, from the original gradients. The second derivative operation, for example, generates, at once, both a sharper and a higher amplitude signal than that produced by the first differentiation. Therefore, when the second derivative signal is subtracted, the resulting edge-gradients are steeper and the density range from the top to the bottom of the edge-gradients is increased over that obtained from the first derivative operation. When the first and second derivatives are combined, an intermediate level of enhancement would be expected. These predictable results, are in general, confirmed by the effects observable in both of the classes of imagery investigated.

From the results obtained in this investigation, it is concluded that,

(1) Differentiation operations can enhance acutance, resolution, contrast and hence, image quality.

(2) Greatest enhancement effects are realized from operations involving the second derivative correction, alone; however, the combined first and second derivative correction may produce comparable enhancement effects under conditions in which the first derivative component has a small gain relative to the gain of the second derivative component.

(3) Enhancement effects due to the first derivative are substantially less than those produced by the other differentiation operations.

Note that the enhancement techniques were evaluated by comparing imagery modified by differentiation with imagery lacking such modification, but which had otherwise been subjected to the same scanning, processing and display conditions. This form of comparison—rather than a comparison of the differentiated

imagery with the original image which was scanned—was selected to obtain a
pure evaluation of the effects of the differentiation operations. Had the
second form of comparison been chosen, the differentiation effects would have
been contaminated by the scanning, processing, and display aspects of the
system. In addition, it was not considered desirable to develop the necessary
apparatus by which enhancement of original imagery could be accomplished,
until the validity of the enhancement techniques could first be demonstrated.

Now that the efficacy of the techniques has been established, subsequent
effort will be directed toward obtaining apparatus which will permit enhance-
ment of original imagery. Paralleling this effort will be an investigation of
the effects of the differentiation operations on human target identification
performance; the aim of this program will be to quantitatively assess the
extent of improvement in speed, accuracy and completeness of information extrac-
tion which can be realized from the use of the enhancement techniques illustrated
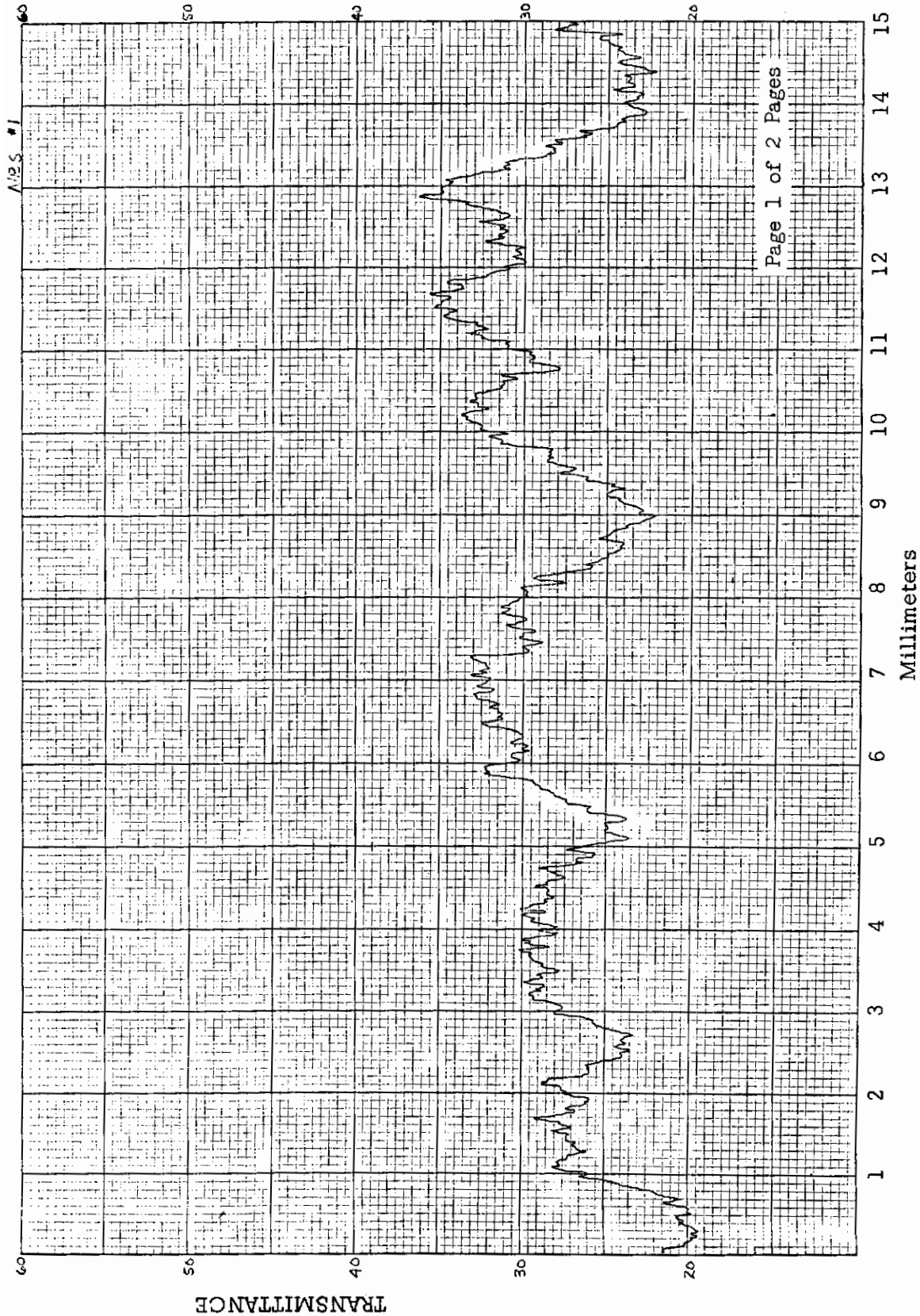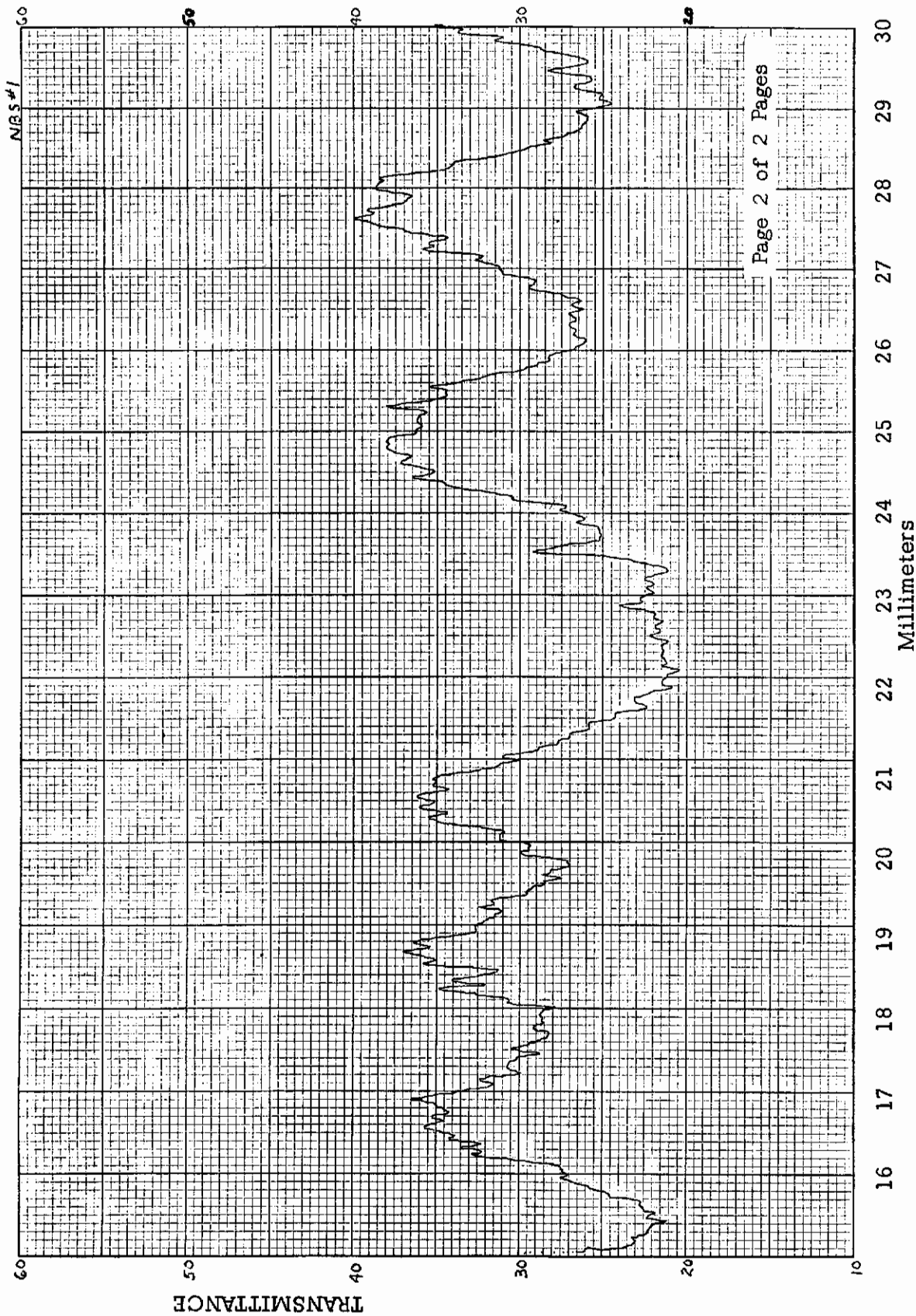in this study.

APPENDIX
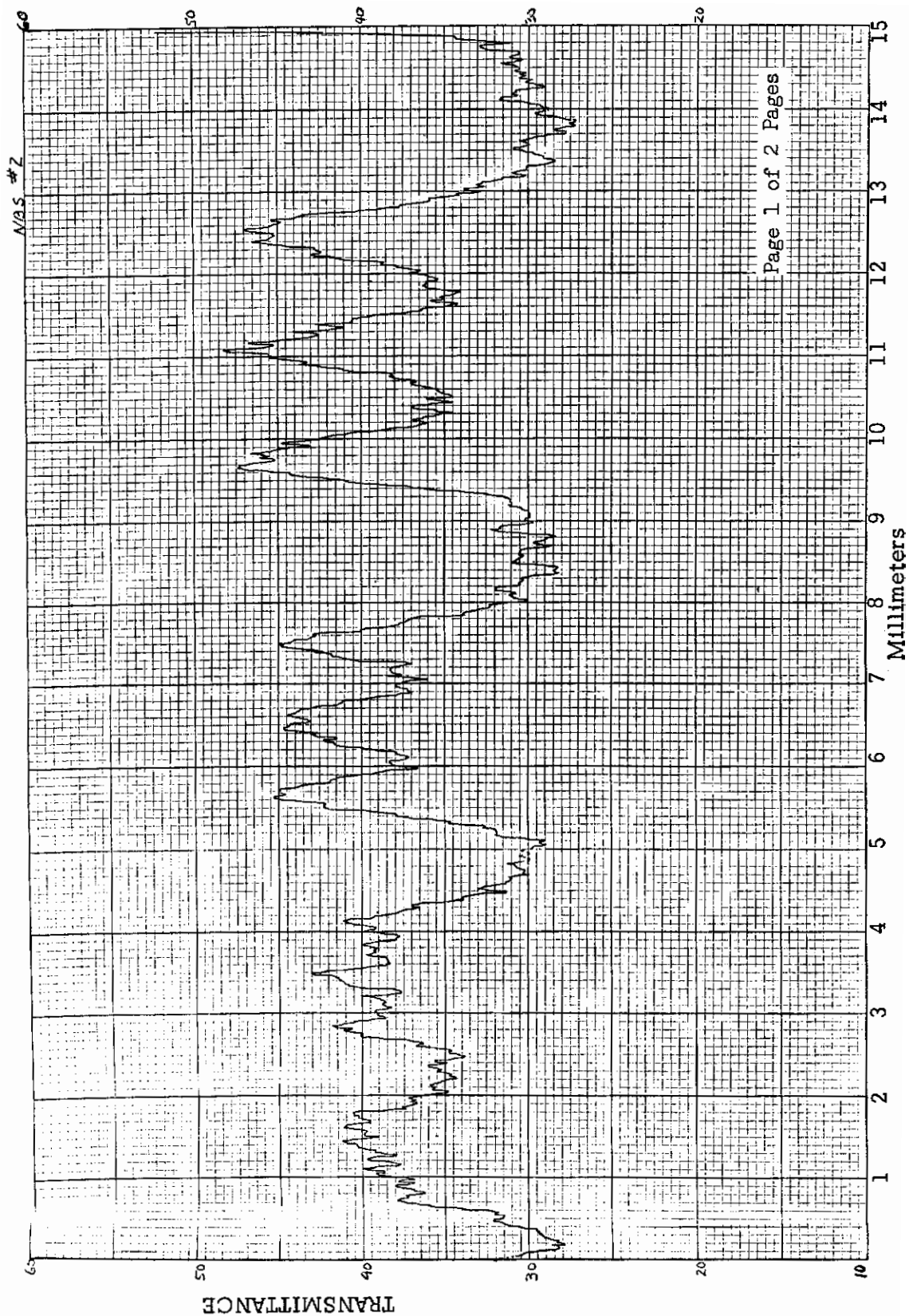
TRANSMITTANCE RECORDINGS

This appendix contains the transmittance recordings obtained from the NBS charts and sine-wave patterns presented in figures 11 and 13, respectively. Each recording bears a number in the upper right corner which indicates the photograph from which the recording was obtained.
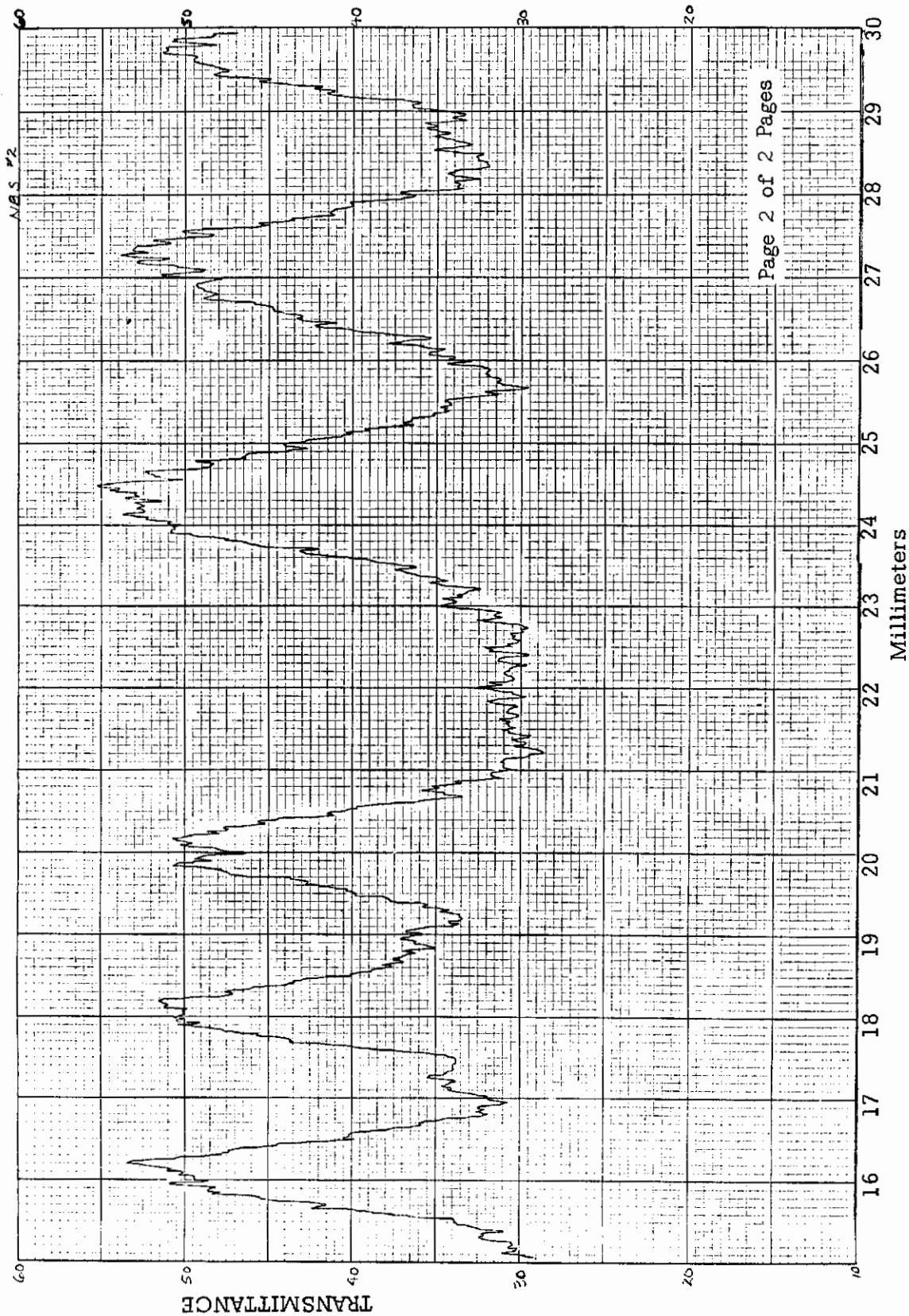
It can be noted from the transmission recordings that the processed image of the sine-wave patterns is distorted under all processing conditions, ie, the transmission pattern is no longer sine in form. This distortion is introduced principally by (1) the nonlinear transformation which occurs from the monitor grid to the phosphor screen* and (2) the nonlinearities in the photographic process involved in obtaining a picture of the television image. Input-output measurements (eg, figures 9 and 10) indicate that only minor distortions of a sine signal are introduced by the system, prior to the monitor grid.
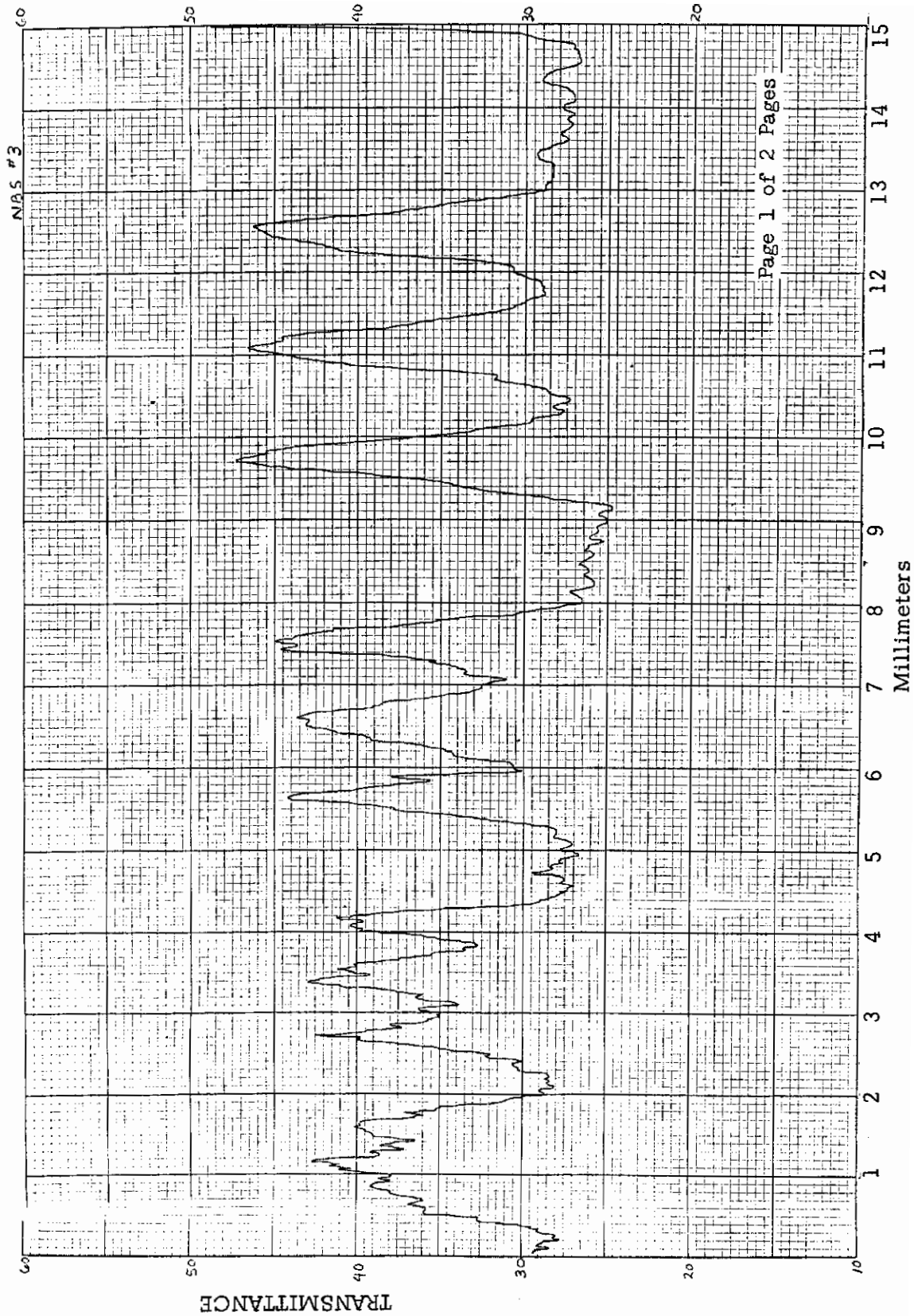

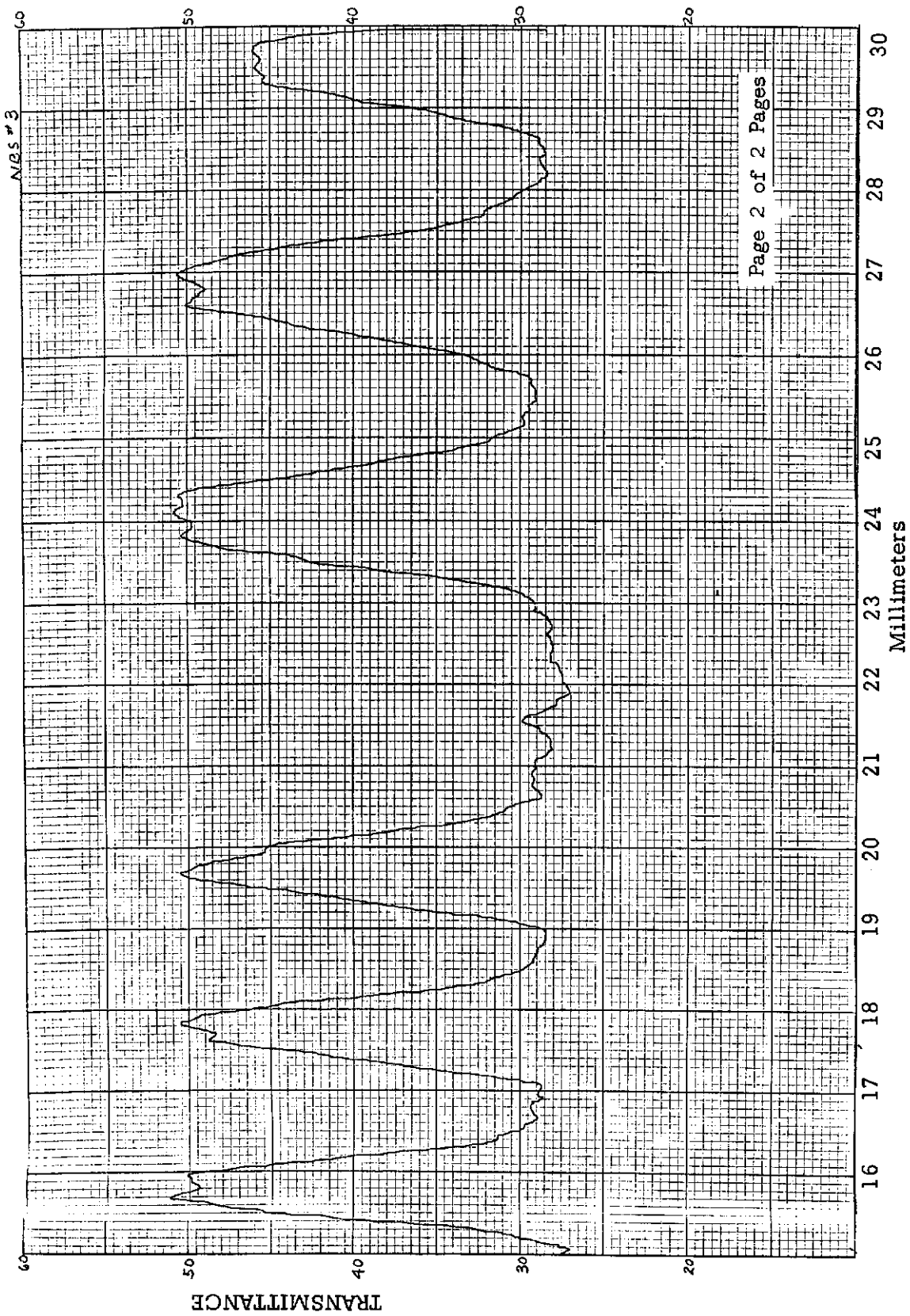*See Fink, D.G., Television Engineering Handbook, McGraw-Hill, Inc., 1957.
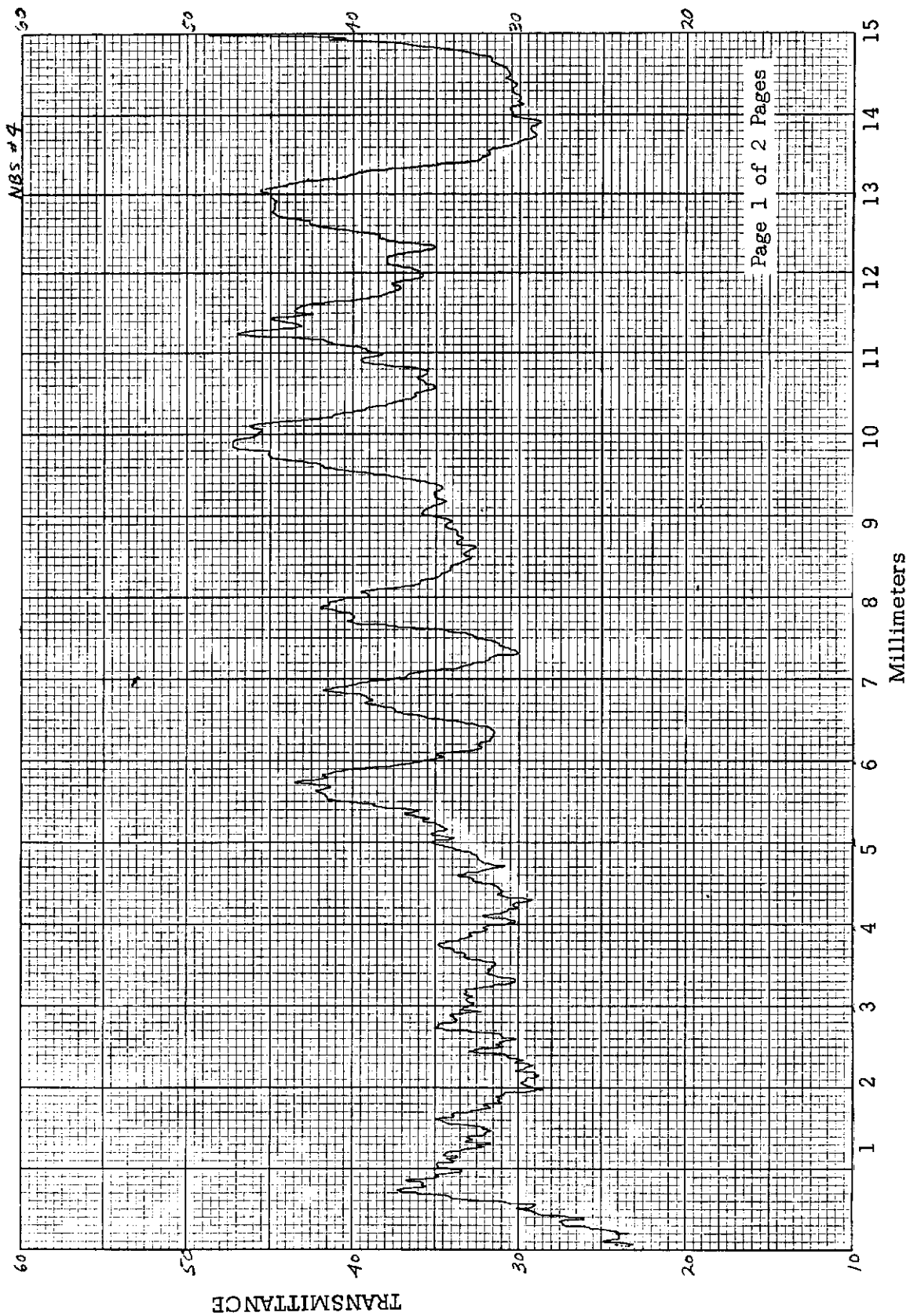
Page 1 of 2 Pages

Millimeters

TRANSMITTANCE

35

NBS #1

TRANSMITTANCE

Millimeters

Page 2 of 2 Pages

36

N/35 #2

Page 1 of 2 Pages

Millimeters

TRANSMITTANCE

37

NAS #3

Page 1 of 2 Pages

TRANSMITTANCE

Millimeters

NBS #4

Page 1 of 2 Pages

Millimeters

TRANSMITTANCE

41

NBS #4

Page 2 of 2 Pages

Millimeters

TRANSMITTANCE

42

NBS #5

Millimeters

TRANSMITTANCE

43

NBS #5

Page 2 of 2 Pages

Millimeters

TRANSMITTANCE

44

SW # 1

TRANSMITTANCE

Millimeters

45

SW # 1

Millimeters

TRANSMITTANCE

46

SW # 2

Millimeters

TRANSMITTANCE

47

SW # 2

Page 2 of 2 Pages

TRANSMITTANCE

Millimeters

48

Millimeters

TRANSMITTANCE

Sw # 2

49

SW #3

Millimeters

TRANSMITTANCE

50

Millimeters

TRANSMITTANCE

SW # 4

51

Page 2 of 2 Pages

SW # 4

Millimeters

TRANSMITTANCE

SW#5

TRANSMITTANCE

Millimeters

53

SW #5

TRANSMITTANCE

Millimeters

LIST OF REFERENCES

1. v. Bekesy, G., "Neural Inhibitory Units of the Eye and Skin: Quantitative Description of Contrast Phenomena," J. Opt. Soc. Am., 50: 1060-1070, 1960.

2. Bliss, J.C., and W.B. Macurdy, "Linear Models for Contrast Phenomena," J. Opt. Soc. Am., 51: 1373-1379, 1961.

3. Cornsweet, T.N., "Determination of the Stimuli for Involuntary Drifts and Saccadic Eye Movements," J. Opt. Soc. Am., 46: 987-993, 1956.

4. Ditchburn, R.W., and B.L. Ginsborg, "Involuntary Eye Movements During Fixation," J. Physiol., 119: 1-17, 1953.

5. Enoch, J.M. "Natural Tendencies in Visual Search of a Complex Display," Visual Search Techniques, A. Morris, and E.A. Horne (Eds), National Academy of Science, National Research Council, Publication 712, 1960.
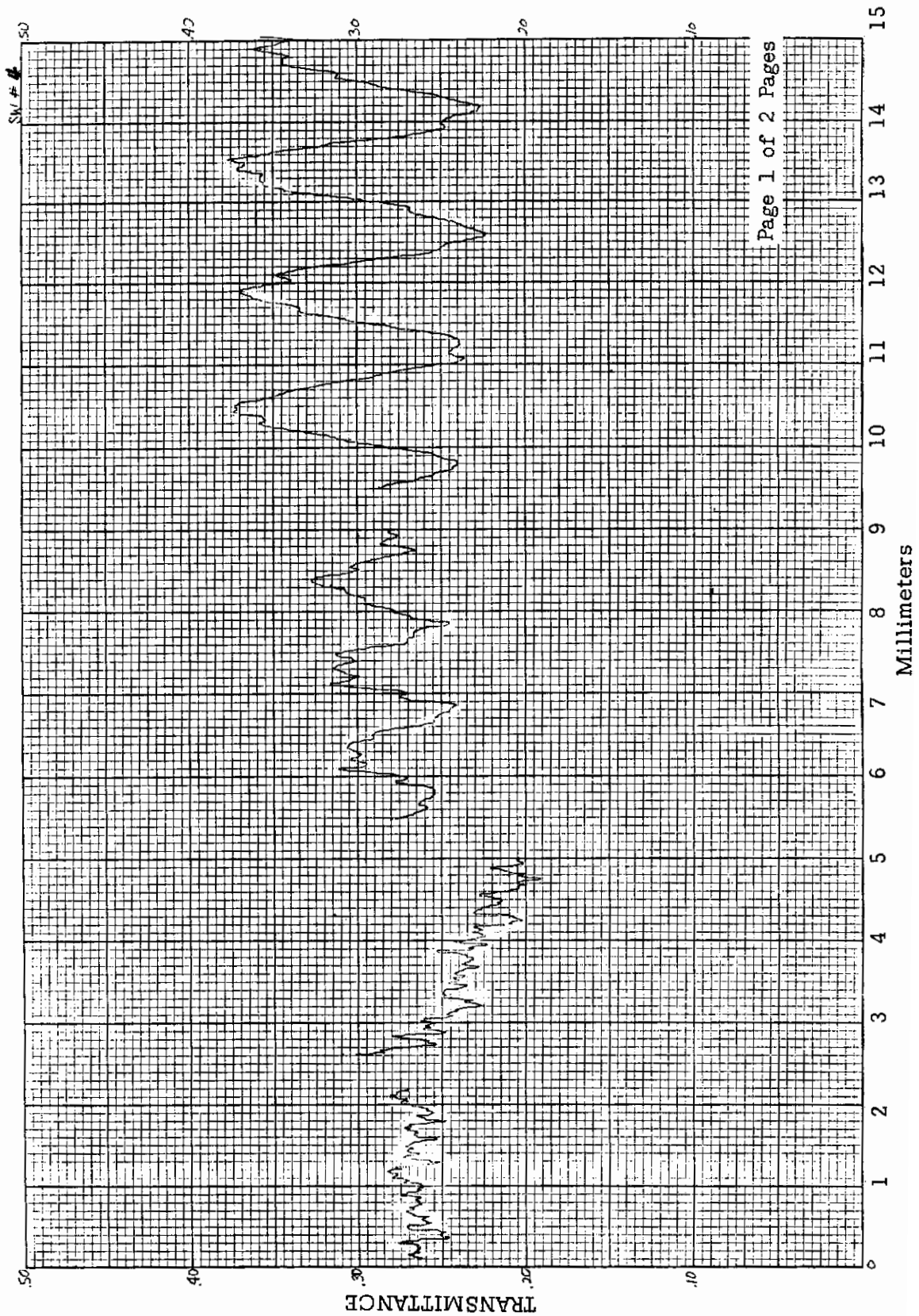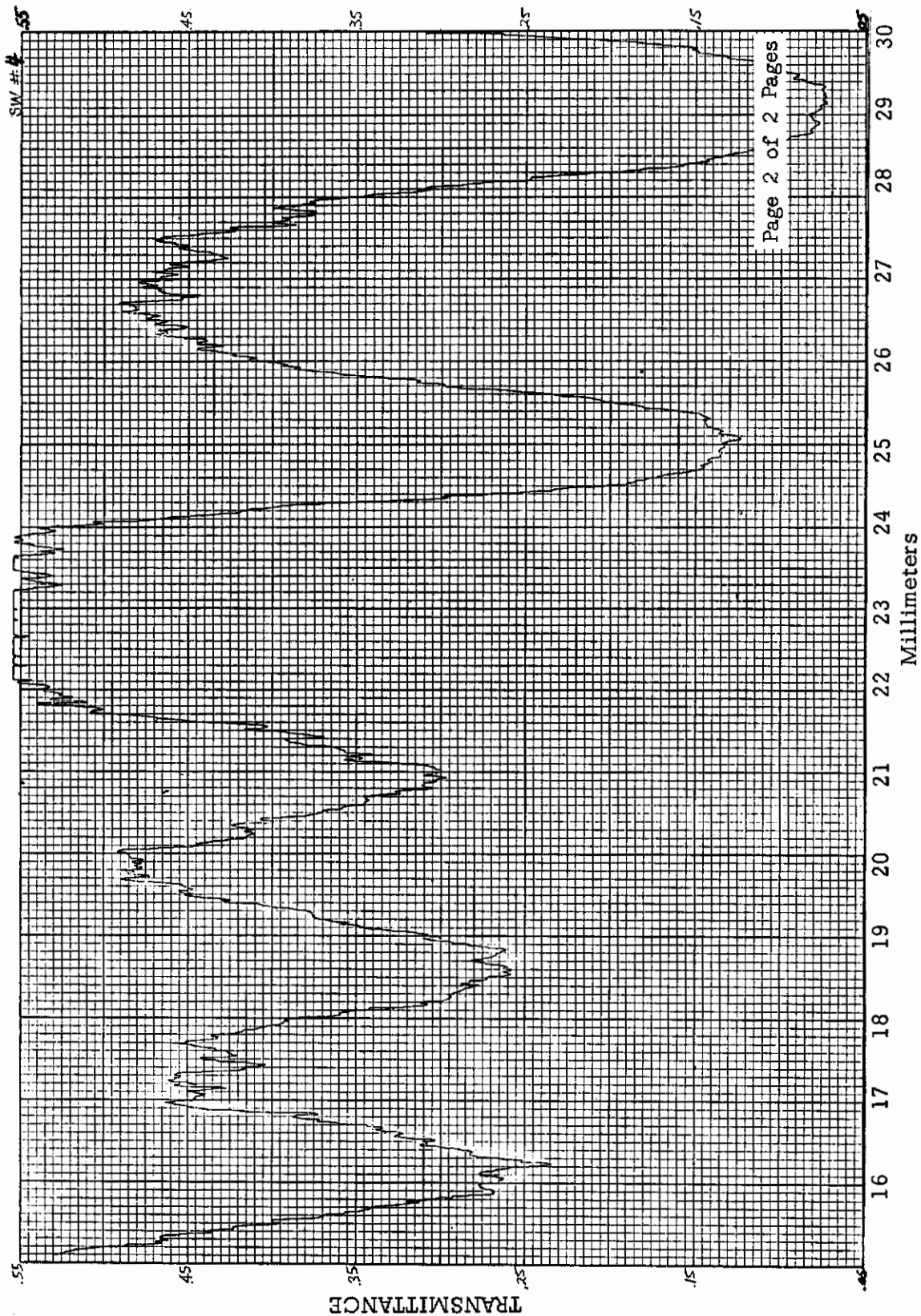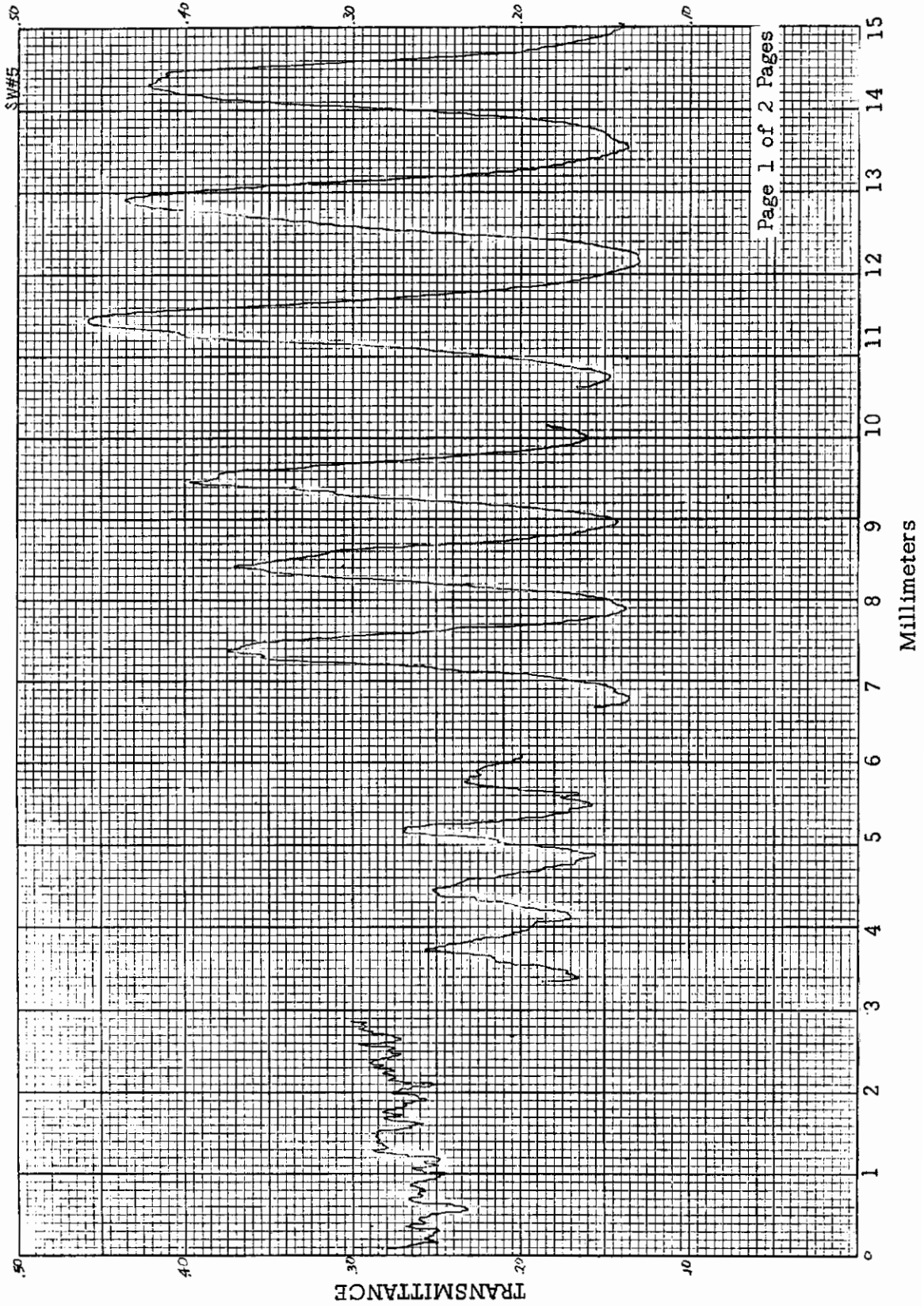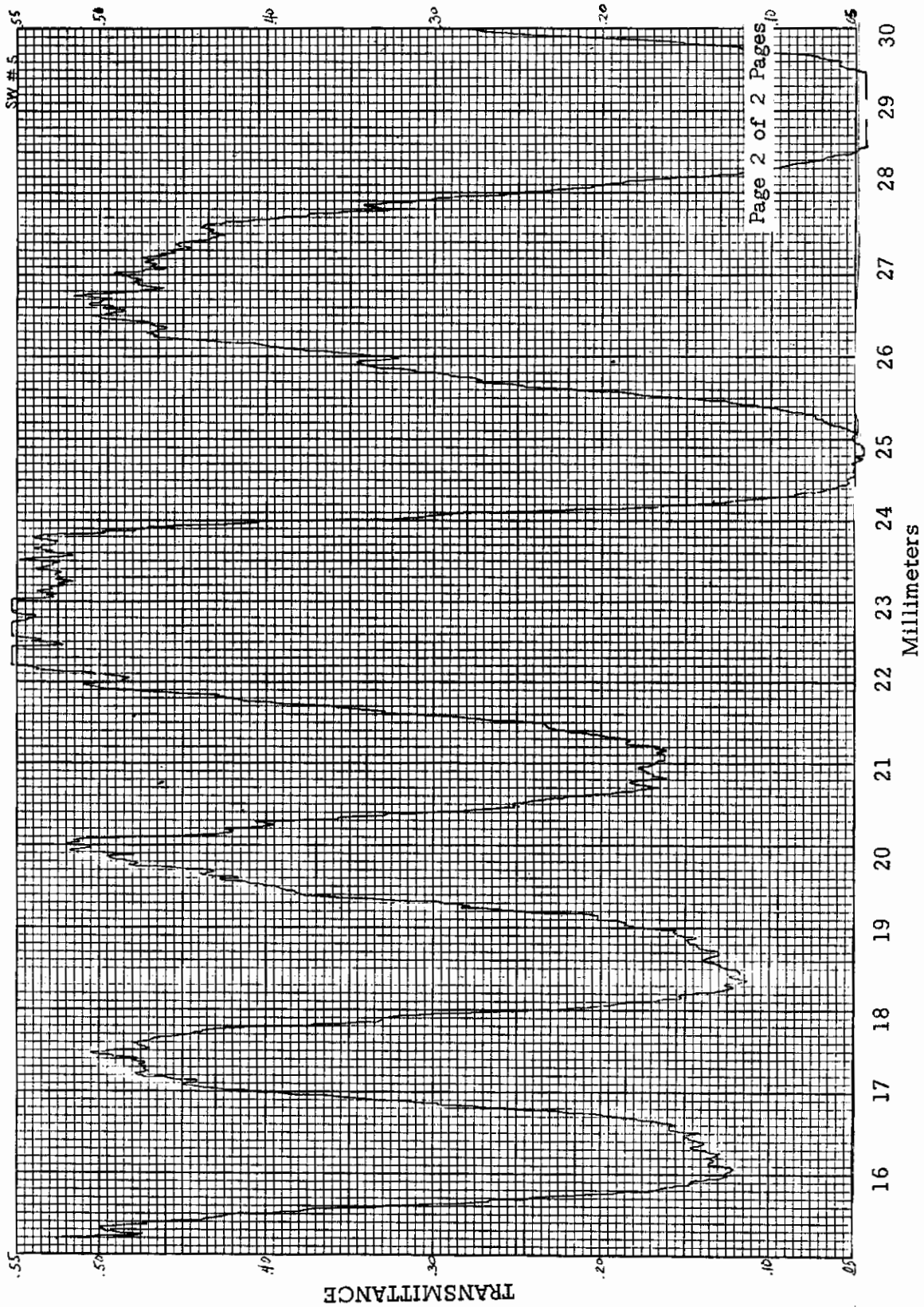
6. Enoch, J.M., The Effect of Image Degradation on Visual Search: Blur, RADC-Technical Note 59-63, 1958.

7. Fiorentini, A., "Dynamic Characteristics of Visual Process," Progress in Optics, Vol I (Ed. E. Wolfe), North Holland Publishing Company, 1961.

8. Fox, W.R., "Visual Discrimination as a Function of Stimulus Size Shape and Edge-Gradient," Form Discrimination as Related to Military Problems, pp 168-175, J.W. Wulfeck, and J.H. Taylor (Eds) National Academy of Science, National Research Council, Publication 561, Washington, D.C., 1957.

9. Fry, G.A., "Mechanisms Subserving Simultaneous Brightness Contrast," Amer. J. Opt. and Arch. of Amer. Acad. Opt., 25 No. 4: 162-178, 1948.

10. Fry, G.A., and J.M. Enoch, The Relation of Blur and Grain to the Visibility of Contrast Borders and Gratings, RADC-Technical Note 58-237, 1959.

11. Green, P.H., Factors in Visual Acuity, Aeromedical Division, USAF Office of Scientific Research, Washington, D.C., 1958.

12. Higgins, G.C., and L.A. Jones, "The Nature and Evaluation of the Sharpness of Photographic Images," J. SMPTE, 58: 277-290, 1952.

13. Higgins, G.C., and R.N. Wolfe, "The Relation of Definition to Sharpness and Resolving Power in a Photographic System," J. Opt. Soc. Am., 45: 121-129, 1955.

14. Howell, W.C., and C.L. Kraft, <u>Size, Blur, and Contrast as Variables</u> <u>Affecting the Legibility of Alpha-Numeric Symbols on Radar-Type</u> <u>Displays</u>, Wright Air Development Center Technical Report 59-536, Wright-Patterson Air Force Base, Ohio, 1959.

15. Kovasznay, L.S.G., and H.M. Joseph, "Image Processing," <u>Proc. IRE,</u> <u>43 No. 2</u>: 560-570, 1955.

16. Krauskopf, J., "Effects of Retinal Image Motion on Contrast Thresholds for Maintained Vision," <u>J. Opt. Soc. Am.</u>, <u>47</u>: 740-744, 1957.

17. Lowry, E.M. and J.J. DePalma, "Sine-Wave Response of the Visual System, I. The Mach Phenomenon," <u>J. Opt. Soc. Am.</u>, <u>51</u>: 740-746, 1961.

18. Ludvigh, E., <u>Perception of Contour: II. Effect of Rate of Change of</u> <u>Retinal Intensity Gradient</u>, U.S. Nav. School of Aviation Med. and Kresge Eye Institute, Joint Project Report No. 5, 1953.

19. Mach, E., <u>The Analysis of Sensations</u>, Dover, 1959.

20. O'Brien, V., "Contour Perception, Illusion and Reality," <u>J. Opt. Soc.</u> <u>Am.</u>, <u>48</u>: 112-119, 1958.

21. Perrin, F.H., "Methods of Appraising Photographic Systems, Part I - Historical Review,: <u>J. SMPTE</u>, 69: 151-156, 1960.

22. Ratliff, F., "Inhibitory Interaction and the Detection and Enhancement of Contours," <u>Sensory Communication</u>, (Ed. W.A. Rosenblith), Wiley, 1961.

23. Riggs, L.A., "Letters," <u>Scient. Am.</u>, 16-18, November 1960.

24. Riggs, L.A., et al., "The Disappearance of Steadily Fixated Visual Test Objects," <u>J. Opt. Soc. Am.</u>, <u>43</u>: 495-501, 1953.

25. Schade, O.H., "A New System of Measuring and Specifying Image Definition," <u>Optical Image Evaluation</u>, U.S. Dept. of Commerce, NBS, Washington, D.C., Circular 526, 1954.

26. Stulz, K.F. and H.J. Zweig, "Roles of Sharpness and Graininess in Photographic Quality and Definition," <u>J. Opt. Soc. Am.</u>, <u>52</u>: 45-50, 1962.

27. Westheimer, G., and F.W. Campbell, "Light Distribution in the Image Formed by the Living Human Eye," <u>J. Opt. Soc. Am.</u>, <u>52</u>: 1040-1045, 1962.

28. Wolfe, R.N., "Width of the Human Visual Spread Function as Determined Psychometrically," <u>J. Opt. Soc. Am.</u>, <u>52</u>: 460-469, 1962.

DOCUMENT CONTROL DATA - R&D		
(Security classification of title, body of abstract and indexing annotation must be entered when the overall report is classified)		

1. ORIGINATING ACTIVITY *(Corporate author)*	2a. REPORT SECURITY CLASSIFICATION
North American Aviation Incorporated Advanced Systems Research Columbus, Ohio	UNCLASSIFIED
	2b. GROUP N/A

3. REPORT TITLE

IMAGE QUALITY ENHANCEMENT

4. DESCRIPTIVE NOTES *(Type of report and inclusive dates)*

Final report, December 1962 – February 1964

5. AUTHOR(S) *(Last name, first name, initial)*

Brainard, Robert W.
Ornstein, George N., PhD

6. REPORT DATE	7a. TOTAL NO. OF PAGES	7b. NO. OF REFS
April 1965	56	28

8a. CONTRACT OR GRANT NO. AF 33(616)-7996	9a. ORIGINATOR'S REPORT NUMBER(S)
b. PROJECT NO 7183	
c. Task No. 718302	9b. OTHER REPORT NO(S) *(Any other numbers that may be assigned this report)*
d.	AMRL-TR-65-28

10. AVAILABILITY/LIMITATION NOTICES

Qualified requesters may obtain copies of this report from DDC.
Available, for sale to the public, from the Clearinghouse for Federal Scientific and
Technical Information, CFSTI (formerly OTS), Sills Bldg, Springfield, Virginia 22151

11. SUPPLEMENTARY NOTES	12. SPONSORING MILITARY ACTIVITY
	Aerospace Medical Research Laboratories, Aerospace Medical Division, Air Force Systems Command, Wright-Patterson AFB, Ohio

13. ABSTRACT

A technique for enhancing the quality of imagery was investigated. The technique consists of obtaining a video signal from a transparency and adding to this signal its first and/or second derivative(s). The efficacy of the technique was evaluated by comparing imagery produced by the video signal and its derivative(s) with imagery produced by the video signal alone. The imagery investigated consisted of standard test patterns and aerial photographs. The processed test patterns were quantitatively analyzed to determine the resolution, contrast and acutance of the imagery. The results indicate: (1) differentiation enhances image quality, as indicated by the resolution, contrast and acutance metrics, (2) greatest enhancement is produced by operations which include second-order differentiation, and (3) the least enhancement is produced by first-order differentiation. The aerial photographic imagery shows the same enhancing effects as those obtained with the test patterns.

DD FORM 1 JAN 64 **1473**

AF-WP-B-AUG 64   400

14. KEY WORDS	LINK A		LINK B		LINK C	
	ROLE	WT	ROLE	WT	ROLE	WT
Photographic reconnaissance						
Aerial photography						
Display systems						
Visual perception						
Intelligibility						
Visibility						
Images						
Photographic images						
Video signals						

INSTRUCTIONS

1. ORIGINATING ACTIVITY: Enter the name and address of the contractor, subcontractor, grantee, Department of Defense activity or other organization *(corporate author)* issuing the report.

2a. REPORT SECURITY CLASSIFICATION: Enter the overall security classification of the report. Indicate whether "Restricted Data" is included. Marking is to be in accordance with appropriate security regulations.

2b. GROUP: Automatic downgrading is specified in DoD Directive 5200.10 and Armed Forces Industrial Manual. Enter the group number. Also, when applicable, show that optional markings have been used for Group 3 and Group 4 as authorized.

3. REPORT TITLE: Enter the complete report title in all capital letters. Titles in all cases should be unclassified. If a meaningful title cannot be selected without classification, show title classification in all capitals in parenthesis immediately following the title.

4. DESCRIPTIVE NOTES: If appropriate, enter the type of report, e.g., interim, progress, summary, annual, or final. Give the inclusive dates when a specific reporting period is covered.

5. AUTHOR(S): Enter the name(s) of author(s) as shown on or in the report. Enter last name, first name, middle initial. If military, show rank and branch of service. The name of the principal author is an absolute minimum requirement.

6. REPORT DATE: Enter the date of the report as day, month, year; or month, year. If more than one date appears, on the report, use date of publication.

7a. TOTAL NUMBER OF PAGES: The total page count should follow normal pagination procedures, i.e., enter the number of pages containing information.

7b. NUMBER OF REFERENCES: Enter the total number of references cited in the report.

8a. CONTRACT OR GRANT NUMBER: If appropriate, enter the applicable number of the contract or grant under which the report was written.

8b, 8c, & 8d. PROJECT NUMBER: Enter the appropriate military department identification, such as project number, subproject number, system numbers, task number, etc.

9a. ORIGINATOR'S REPORT NUMBER(S): Enter the official report number by which the document will be identified and controlled by the originating activity. This number must be unique to this report.

9b. OTHER REPORT NUMBER(S): If the report has been assigned any other report numbers *(either by the originator or by the sponsor)*, also enter this number(s).

10. AVAILABILITY/LIMITATION NOTICES: Enter any limitations on further dissemination of the report, other than those imposed by security classification, using standard statements such as:

(1) "Qualified requesters may obtain copies of this report from DDC."

(2) "Foreign announcement and dissemination of this report by DDC is not authorized."

(3) "U. S. Government agencies may obtain copies of this report directly from DDC. Other qualified DDC users shall request through

_____ ."

(4) "U. S. military agencies may obtain copies of this report directly from DDC. Other qualified users shall request through

_____ ."

(5) "All distribution of this report is controlled. Qualified DDC users shall request through

_____ ."

If the report has been furnished to the Office of Technical Services, Department of Commerce, for sale to the public, indicate this fact and enter the price, if known.

11. SUPPLEMENTARY NOTES: Use for additional explanatory notes.

12. SPONSORING MILITARY ACTIVITY: Enter the name of the departmental project office or laboratory sponsoring *(paying for)* the research and development. Include address.

13. ABSTRACT: Enter an abstract giving a brief and factual summary of the document indicative of the report, even though it may also appear elsewhere in the body of the technical report. If additional space is required, a continuation sheet shall be attached.

It is highly desirable that the abstract of classified reports be unclassified. Each paragraph of the abstract shall end with an indication of the military security classification of the information in the paragraph, represented as *(TS)*, *(S)*, *(C)*, or *(U)*

There is no limitation on the length of the abstract. However, the suggested length is from 150 to 225 words.

14. KEY WORDS: Key words are technically meaningful terms or short phrases that characterize a report and may be used as index entries for cataloging the report. Key words must be selected so that no security classification is required. Identifiers, such as equipment model designation, trade name, military project code name, geographic location, may be used as key words but will be followed by an indication of technical context. The assignment of links, rules, and weights is optional.